JCTC Journal of Chemical Theory and Computation

ARTICLE

pubs.acs.org/JCTC

Embedding vs Supermolecular Strategies in Evaluating the Hydrogen-Bonding-Induced Shifts of Excitation Energies

Georgios Fradelos,[†] Jesse J. Lutz,[‡] Tomasz A. Wesołowski,[*,†] Piotr Piecuch,[*,‡] and Marta Włoch[§]

[†]Département de Chimie Physique, Université de Genève, 30, quai Ernest-Ansermet, CH-1211 Genève 4, Switzerland

[‡]Department of Chemistry, Michigan State University, East Lansing, Michigan 48824, United States

[§]Department of Chemistry, Michigan Technological University, Houghton, Michigan 49931, United States

Supporting Information

ABSTRACT: Shifts in the excitation energy of the organic chromophore, *cis*-7-hydroxyquinoline (*cis*-7HQ), corresponding to the $\pi \rightarrow \pi^*$ transition in *cis*-7HQ and induced by the complexation with a variety of small hydrogen-bonded molecules, obtained with the frozen-density embedding theory (FDET), are compared with the results of the supermolecular equation-of-motion coupled-cluster (EOMCC) calculations with singles, doubles, and noniterative triples, which provide the reference theoretical data, the supermolecular time-dependent density functional theory (TDDFT) calculations, and experimental spectra. Unlike in the supermolecular EOMCC and TDDFT cases, where each complexation-induced spectral shift is evaluated by performing two separate calculations, one for the complex and another one for the isolated chromophore, the FDET shifts are evaluated as the differences of the excitation energies determined for the same many-electron system, representing the chromophore fragment with two different effective potentials. By considering eight complexes of *cis*-7HQ with up to three small hydrogen-bonded molecules, it is shown that the spectral shifts resulting from the FDET calculations employing nonrelaxed environment densities and their EOMCC reference counterparts are in excellent agreement with one another, whereas the analogous shifts obtained with the supermolecular TDDFT method do not agree with the EOMCC reference data. The average absolute deviation between the complexation-induced shifts, which can be as large, in absolute value, as about 2000 cm^{-1}, obtained using the nonrelaxed FDET and supermolecular EOMCC approaches that represent two entirely different computational strategies, is only about 100 cm^{-1}, i.e., on the same order as the accuracy of the EOMCC calculations. This should be contrasted with the supermolecular TDDFT calculations, which produce the excitation energy shifts that differ from those resulting from the reference EOMCC calculations by about 700 cm^{-1} on average. Among the discussed issues are the choice of the electronic density defining the environment with which the chromophore interacts, which is one of the key components of FDET considerations, the basis set dependence of the FDET, supermolecular TDDFT, and EOMCC results, the usefulness of the monomer vs supermolecular basis expansions in FDET considerations, and the role of approximations that are used to define the exchange-correlation potentials in FDET and supermolecular TDDFT calculations.

1. INTRODUCTION

Accurately predicting the effect of a hydrogen-bonded environment on the electronic structure of embedded molecules represents a challenge for computational chemistry. In spite of being relatively weak, noncovalent interactions with the environment, such as hydrogen bonds, can qualitatively affect the electronic structure and properties of the embedded molecules. Among such properties, electronic excitation energies are of great interest in view of the common use of organic chromophores as probes in various environments.[1−4] Typically, hydrogen bonding results in shifts in the positions of the maxima of the absorption and emission bands anywhere between a few hundred and about 3000 cm^{-1}.[5] Thus, in order to be able to use computer modeling for the interpretation of experimental data, the intrinsic errors of the calculated shifts must be very small, on the order of 100 cm^{-1} or less.

Unfortunately, the brute force application of the supermolecular strategy to an evaluation of the excitation energy shifts due to the formation of weakly bound complexes with environment molecules, in which one determines the shift as a difference between the excitation energy for a given electronic transition in the complex and the analogous excitation energy characterizing the isolated chromophore, has a limited range of applicability. The supermolecular approach hinges on a condition that many of the existing quantum chemistry approaches struggle with, namely, the ability of a given electronic structure method to provide an accurate and well-balanced description of excitation energies in systems that have different sizes, which in the specific case of spectral shifts induced by complexation are the total system consisting of the chromophore and environment molecules and the system representing the isolated chromophore. *Ab initio* methods based on the equation-of-motion (EOM)[6−10] or linear-response[11−16] coupled-cluster (CC)[17−22] theories (cf. refs 23−25 for selected reviews), including, among many schemes proposed to date, the basic EOMCC approach with singles and doubles (EOMCCSD)[7−9] and the suitably modified variant of the completely renormalized (CR) EOMCC theory with singles, doubles, and noniterative triples, abbreviated as δ-CR-EOMCC(2,3), which is based on the CR-CC(2,3)[26−28] and CR-EOMCC(2,3)[29,30]

Received: February 10, 2011
Published: May 02, 2011

methods and which is used in the present study to provide the reference data, or the closely related EOMCCSD$(2)_T$[31] and EOMCCSD$(\tilde{T})$[32] approximations, satisfy this condition, since they provide an accurate and systematically improvable description of the electronic excitations in molecular systems and satisfy the important property of size-intensivity,[16,33] but their applicability is limited to relatively small molecular problems due to the CPU steps that typically scale as $\mathcal{N}^6$–$\mathcal{N}^7$ with the system size $\mathcal{N}$. In recent years, progress has been made toward extending the EOMCC and response CC methods to larger molecules through the use of local correlation techniques[34−37] and code parallelization, combined, in analogy to the widely used QM/MM techniques, with molecular mechanics,[38−42] and we hope to be able to extend our own, recently developed, local correlation cluster-in-molecule CC algorithms[43−45] to excited states as well, but in spite of these advances, none of the resulting approaches is as practical, as far as computer costs are concerned, as methods based on the time-dependent density functional theory (TDDFT).[46] Unfortunately, the existing TDDFT approaches, although easily applicable to large molecular systems due to low computer costs, are often not accurate enough to guarantee a robust description of the complexation-induced spectral shifts in weakly bound complexes when the supermolecular approach is employed, due to their well-known difficulties with describing dispersion and charge-transfer interactions, and other intrinsic errors.

Methods employing the embedding strategy, including those based on the frozen-density embedding theory (FDET)[47−50] that interests us in this work, provide an alternative strategy to the supermolecular approach for evaluating the excitation energy shifts. In embedding methods, of both empirical (QM/MM, for instance) and FDET types, the effect of the environment is not treated explicitly but, rather, by means of the suitably designed embedding potential. Thus, instead of solving the electronic Schrödinger equation for the total $(N_A + N_B)$-electron system AB consisting of the N_A-electron chromophore A and N_B-electron environment B, i.e.

$$\hat{H}^{(AB)}|\Psi^{(AB)}\rangle = E^{(AB)}|\Psi^{(AB)}\rangle \tag{1}$$

where $\hat{H}^{(AB)}$ is the Hamiltonian of the total system AB, and the electronic Schrödinger equation for the isolated chromophore A

$$\hat{H}^{(A)}|\Psi^{(A)}\rangle = E^{(A)}|\Psi^{(A)}\rangle \tag{2}$$

where $\hat{H}^{(A)}$ is the Hamiltonian of the chromophore in the absence of environment, and then calculating the shift in an observable of interest associated with an operator $\hat{O}$ by forming the difference of the expectation values of $\hat{O}$ computed for two systems that have different numbers of electrons,

$$\Delta\langle\hat{O}\rangle = \langle\Psi^{(AB)}|\hat{O}|\Psi^{(AB)}\rangle - \langle\Psi^{(A)}|\hat{O}|\Psi^{(A)}\rangle \tag{3}$$

as one would have to do in supermolecular calculations, one solves two many-electron problems characterized by the same number of electrons, namely, eq 2 and

$$[\hat{H}^{(A)} + \hat{V}^{(A)}_{\mathrm{emb}}]|\Psi^{(A)}_{\mathrm{emb}}\rangle = E^{(A)}_{\mathrm{emb}}|\Psi^{(A)}_{\mathrm{emb}}\rangle \tag{4}$$

where $|\Psi^{(A)}_{\mathrm{emb}}\rangle$ is the auxiliary N_A-electron wave function describing the effective state of the chromophore A in the presence of environment B and $\hat{V}^{(A)}_{\mathrm{emb}} = \sum_{i=1}^{N_A} v_{\mathrm{emb}}(\vec{r}_i)$ is the suitably designed embedding operator defined in terms of the effective one-electron potential $v_{\mathrm{emb}}(\vec{r})$. As a result, the complexation-induced shift in an observable represented by an operator $\hat{O}$ is evaluated in the embedding strategy as

$$\Delta\langle\hat{O}\rangle = \langle\Psi^{(A)}_{\mathrm{emb}}|\hat{O}|\Psi^{(A)}_{\mathrm{emb}}\rangle - \langle\Psi^{(A)}|\hat{O}|\Psi^{(A)}\rangle \tag{5}$$

i.e., by using the many-electron wave functions $|\Psi^{(A)}\rangle$ and $|\Psi^{(A)}_{\mathrm{emb}}\rangle$ that represent two different physical states of system A corresponding to the same number of electrons, the state of the isolated chromophore A and the state of A embedded in the environment B. This has two immediate advantages over the supermolecular approach. First, the embedding strategy does not require the explicit consideration of the total $(N_A + N_B)$-electron system consisting of the interacting complex of chromophore and environment. This may lead to a significant cost reduction in the computer effort in applications involving larger environments. Second, by determining the complexation-induced shift $\Delta\langle\hat{O}\rangle$ using the wave functions $|\Psi^{(A)}\rangle$ and $|\Psi^{(A)}_{\mathrm{emb}}\rangle$ corresponding to the same number of electrons, the errors due to approximations used to solve the N_A-electron problems represented by eqs 2 and 4 largely cancel out, as we do not have to worry too much about the possible dependence of the error on the system size. In the calculations of the shifts in excitation energies using the size-intensive EOMCC methods, one does not have to worry about the size dependence of the error resulting from the calculations either, but the supermolecular EOMCC approach requires an explicit consideration of the $(N_A + N_B)$-electron system consisting of the chromophore and environment, which may lead to a significant cost increase when N_B is larger.

The above description implies that the accuracy of the complexation-induced shifts obtained in embedding calculations largely depends on the quality of the embedding operator $\hat{V}^{(A)}_{\mathrm{emb}}$ or the underlying one-electron potential $v_{\mathrm{emb}}(\vec{r})$ that defines it. Thus, when compared with the supermolecular approach, the challenge is moved from assuring the cancellation of errors in approximate solutions of two Schrödinger equations for systems that differ in the number of electrons to developing a suitable form of the embedding potential that can accurately describe the state of the chromophore in the weakly bound complex with environment. As already mentioned above, the practical advantage of the embedding strategy (provided a sufficiently accurate approximation for the embedding potential is employed) is the fact that it can be used for much larger systems than the supermolecular one and can even be applied in multiscale molecular simulations.[48,51−53] As formally demonstrated in our previous studies,[47−50] the embedding operator can be represented in terms of a local potential $v_{\mathrm{emb}}(\vec{r})$ (orbital-free embedding potential), which is determined by the pair of electron densities, ρ_A, describing the embedded system A and constructed using the $|\Psi^{(A)}_{\mathrm{emb}}\rangle$ wave function, and ρ_B, representing the electron density of the environment B. Unfortunately, except for some analytically solvable systems,[54] the precise dependence of $v_{\mathrm{emb}}(\vec{r})$ on ρ_A and ρ_B is not known. Only its electrostatic component is known exactly. The nonelectrostatic component, which arises from the nonadditivity of the density functionals for the exchange-correlation and kinetic energies, must be approximated or reconstructed, either analytically (if possible)[54] or numerically.[55−57] In the case of the hydrogen-bonded environments that interest us in this study, the electrostatic component of the exact embedding potential can be expected to dominate and the overall accuracy of the environment-induced changes of the electronic structure of embedded

species can be expected to be accurately described. Indeed, a number of our previous studies[58,59] show that the currently known approximants to the relevant functional representations of $v_{emb}(\vec{r})$ in terms of ρ_A and ρ_B are adequate.

Our past examinations of the formal and practical aspects of the FDET methodology have largely focused on model systems or direct comparisons with experimental results. Analytically solvable model systems (see ref 54) are especially important, since, as pointed out above, they enable one to develop ideas about the dependence of the embedding potential $v_{emb}(\vec{r})$ on densities ρ_A and ρ_B, but real many-electron systems may be quite different than models. A comparison with experimental results is clearly the ultimate goal of any modeling technique, and FDET is no different in this regard, but it often happens that experiments have their own error bars and their proper interpretation may require additional considerations and the incorporation of physical effects that are not included in the purely electronic structure calculations. This study offers an alternative way of testing the FDET techniques. Thus, the main objective of the present work is to make a direct comparison of the benchmark results obtained in the high-level, supermolecular, wave function-based EOMCC calculations, using the aforementioned size-intensive modification of the CR-EOMCC(2,3) method,[29,30] designated as δ-CR-EOMCC(2,3), with those produced by the embedding-theory-based FDET approach[47−50] and the supermolecular TDDFT methodology. To this end, we obtain the δ-CR-EOMCC(2,3)-based shifts in the vertical excitation energy corresponding to the $\pi \rightarrow \pi^*$ transition in the organic chromophore, *cis*-7-hydroxyquinoline (*cis*-7HQ), induced by formation of hydrogen-bonded complexes with eight different environments defined by the water, ammonia, methanol, and formic acid molecules and their selected aggregates consisting of up to three molecules, for which, as shown in this work, reliable EOMCC data can be generated and which were previously examined using laser resonant two-photon UV spectroscopy,[5,59] and we use the resulting reference shift values to assess the quality of the analogous spectral shifts obtained in the FDET and supermolecular TDDFT calculations.

Having access to accurate reference EOMCC data enables us to explore various aspects of the FDET methodology and approximations imposed within. For example, in addition to the approximations used for the nonelectrostatic component of the embedding potential $v_{emb}(\vec{r})$, the FDET techniques exploit various forms of the electron density of the environment ρ_B. Since ρ_B is an assumed quantity in the FDET considerations, its choice may critically affect the calculated environment-induced shifts in observables.[60,61] The dependence of the FDET values of the shifts in the excitation energy of *cis*-7HQ induced by the complexation with hydrogen-bonded molecules on the form of ρ_B represents one of the most important aspects of the present study. Among other issues discussed in this work are the basis set dependence of the FDET, supermolecular TDDFT, and EOMCC results, the usefulness of the monomer vs supermolecular basis expansions in the FDET calculations, and the role of approximations that are used to define the exchange-correlation potentials in the FDET and supermolecular TDDFT calculations.

Although the main focus of this work is a comparison of the embedding-theory-based FDET and supermolecular TDDFT results with the high-level *ab initio* EOMCC data to demonstrate the advantages of the FDET approach over the conventional supermolecular TDDFT methodology in a realistic application, a comparison of the theoretical shifts with the corresponding experimental data[5,59] is discussed as well. The gas-phase complexes examined in this paper have been intensely studied, both experimentally and theoretically, since some of these complexes, particularly the larger ones, can be viewed as models of proton-transferring chains in biomolecular systems.[1,62]

2. METHODS

As explained in the Introduction, the main goal of this study is a comparison of the shifts in the excitation energy corresponding to the $\pi \rightarrow \pi^*$ transition in the *cis*-7HQ system, induced by the formation of hydrogen-bonded complexes of *cis*-7HQ with a number of small molecules, resulting from the embedding-theory-based FDET approach and supermolecular TDDFT calculations, with those obtained with the EOMCC-based δ-CR-EOMCC(2,3) scheme that provides the theoretical reference data. This section provides basic information about the electronic structure theories exploited in this work. Since the supermolecular TDDFT approach is a well-established methodology, our description focuses on the FDET and EOMCC methods used in our calculations.

2.1. Frozen-Density Embedding Theory. The FDET formalism[47−50,63] provides basic equations for the variational treatment of a quantum-mechanical subsystem embedded in a given electronic density. Various FDET-based approaches developed by us[47−50,54,58,64] and others,[65−69] differing in the way the environment density is generated, the choice made for the approximants for the relevant density functionals, or the choice for the quantum-mechanical descriptors for the embedded subsystem, are in use today. Below, we outline the basic elements of the FDET methodology.

1. Basic Variables. The total system *AB*, consisting of a molecule or an aggregate of molecules of interest, *A*, embedded in the environment *B* created by the other molecule(s), is characterized by two types of densities. The first one is the density of the embedded molecule(s), $\rho_A(\vec{r})$, which is typically represented using one the following auxiliary quantities: (i) the occupied orbitals of a noninteracting reference system $\{\phi_i^{(A)}(\vec{r}), i = 1, ..., N_A\}$,[47] (ii) the occupied and unoccupied orbitals of a noninteracting reference system,[63] (iii) the interacting wave function,[49] or (iv) the one-particle density matrix.[50] The second one is the density of the environment, $\rho_B(\vec{r})$, which is fixed for a given electronic problem ("frozen density").

2. Constrained Search. The optimum density $\rho_A(\vec{r})$ of the system *A* embedded in the environment *B*, represented by the fixed density $\rho_B(\vec{r})$ satisfying

$$\int \rho_B(\vec{r})\, d\vec{r} = N_B \tag{6}$$

is obtained by performing the following constrained search:

$$E_{emb}^{(A)}[\rho_B] = \min_{\rho \geq \rho_B} E_{HK}[\rho] = \min_{\rho_A} E_{HK}[\rho_A + \rho_B] \tag{7}$$

subject to the conditions

$$\int \rho(\vec{r})\, d\vec{r} = N_A + N_B \tag{8}$$

and

$$\int \rho_A(\vec{r})\, d\vec{r} = N_A \tag{9}$$

where $E_{HK}[\rho]$ in eq 7 is the usual Hohenberg−Kohn energy functional.

3. Constrained Search by Modifying the External Potential. In practice, the search for the optimum density ρ_A, defined by eq 7, is conducted by solving eq 4, in which $\hat{H}^{(A)}$ is the environment-free Hamiltonian of the isolated system A and $\hat{V}^{(A)}_{\mathrm{emb}} = \sum_{i=1}^{N_A} v_{\mathrm{emb}}(\vec{r})$, where $\hat{v}_{\mathrm{emb}}(\vec{r})$ has the form of a local, orbital-free, embedding potential $v^{\mathrm{eff}}_{\mathrm{emb}}(\vec{r})$, determined by the pair of densities $\rho_A(\vec{r})$ and $\rho_B(\vec{r})$ and designated by $v^{\mathrm{eff}}_{\mathrm{emb}}[\rho_A,\rho_B;\vec{r}]$.

4. Orbital-Free Embedding Potential. As shown earlier,[49] the relationship between the local potential $v^{\mathrm{eff}}_{\mathrm{emb}}[\rho_A,\rho_B;\vec{r}]$ and densities $\rho_A(\vec{r})$ and $\rho_B(\vec{r})$ depends on the quantum-mechanical descriptors that are used as the auxiliary quantities for defining $\rho_A(\vec{r})$. If we use the orbitals of a noninteracting reference system, the wave function of the full configuration interaction form, or the one-particle density matrix as the descriptors to define $\rho_A(\vec{r})$, the local, orbital-free, embedding potential reads as follows:

$$v^{\mathrm{eff}}_{\mathrm{emb}}[\rho_A,\rho_B;\,\vec{r}] = v^{B}_{\mathrm{ext}}(\vec{r}) + \int \frac{\rho_B(\vec{r}\,')}{|\vec{r}\,' - \vec{r}|}\,\mathrm{d}\vec{r}\,' + v^{\mathrm{nad}}_{\mathrm{xc}}[\rho_A,\rho_B](\vec{r}) + v^{\mathrm{nad}}_{t}[\rho_A,\rho_B](\vec{r}) \quad (10)$$

where

$$v^{\mathrm{nad}}_{\mathrm{xc}}[\rho_A,\rho_B](\vec{r}) = \left.\frac{\delta E_{\mathrm{xc}}[\rho]}{\delta\rho}\right|_{\rho=\rho_A+\rho_B} - \left.\frac{\delta E_{\mathrm{xc}}[\rho]}{\delta\rho}\right|_{\rho=\rho_A} \quad (11)$$

and

$$v^{\mathrm{nad}}_{t}[\rho_A,\rho_B](\vec{r}) = \left.\frac{\delta T_s[\rho]}{\delta\rho}\right|_{\rho=\rho_A+\rho_B} - \left.\frac{\delta T_s[\rho]}{\delta\rho}\right|_{\rho=\rho_A} \quad (12)$$

As we can see, the above equation for $v^{\mathrm{eff}}_{\mathrm{emb}}[\rho_A,\rho_B;\vec{r}]$ involves the external and Coulomb potentials due to the environment B and the $v^{\mathrm{nad}}_{\mathrm{xc}}[\rho_A,\rho_B](\vec{r})$ and $v^{\mathrm{nad}}_{t}[\rho_A,\rho_B](\vec{r})$ components that arise from the nonadditivities of the exchange-correlation and kinetic energy functionals of the Kohn−Sham formulation[70] of DFT,[71] $E_{\mathrm{xc}}[\rho]$ and $T_s[\rho]$, respectively.

5. Kohn−Sham Equations with Constrained Electronic Density. Once $v^{\mathrm{eff}}_{\mathrm{emb}}[\rho_A,\rho_B;\vec{r}]$ is defined, as in eq 10, and if we use a noninteracting reference system to perform the constrained search given by eq 7, the corresponding orbitals $\phi^{(A)}_i$, i = 1, ..., N_A, of the system A embedded in the environment B are obtained from the following Kohn−Sham-like equations [cf. eqs 20 and 21 in our earlier work[47]]:

$$\left[-\frac{1}{2}\nabla^2 + v^{\mathrm{eff}}_{\mathrm{KS}}[\rho_A;\,\vec{r}] + v^{\mathrm{eff}}_{\mathrm{emb}}[\rho_A,\rho_B;\,\vec{r}]\right]\phi^{(A)}_i = \varepsilon^{(A)}_i\phi^{(A)}_i \quad (13)$$

where $v^{\mathrm{eff}}_{\mathrm{KS}}[\rho_A;\vec{r}]$ is the usual expression for the potential of the Kohn−Sham DFT for the isolated system A. After obtaining the orbitals $\phi^{(A)}_i$ and the corresponding orbital energies $\varepsilon^{(A)}_i$ by solving eq 13, we proceed to the determination of the ground- and excited-state energies and properties, which in this case describe the system A embedded in the environment B, in a usual manner, using standard techniques of DFT or TDDFT.

The effectiveness of methods based on eq 13, with $v^{\mathrm{eff}}_{\mathrm{emb}}[\rho_A,\rho_B;\vec{r}]$ determined using eq 10, in the calculations of changes in the electronic structure arising due to the interactions between the embedded system and its environment was demonstrated in a number of applications, including vertical excitation energies,[59,63] ESR hyperfine coupling constants,[72,73] ligand-field splittings of f levels in lanthanide impurities,[60] NMR shieldings,[74] dipole and quadrupole moments, and electronic excitation energies and frequency-dependent polarizabilities.[75] The FDET strategy, as summarized above, is expected to calculate the shifts in the vertical excitation energy corresponding to the $\pi \rightarrow \pi^*$ transition in the *cis*-7HQ system due to its environment in a reasonable manner,[52] and the present paper verifies if this is indeed the case by comparing the results of the FDET and δ-CR-EOMCC(2,3)-based EOMCC calculations.

In this context, it is useful to mention two other approaches related to FDET that aim at the description of a system consisting of subsystems, including the situation of a molecule or a molecular complex embedded in an environment which interests us here, namely, the subsystem formulation of DFT (SDFT)[76,77] and the recently developed partition DFT (PDFT).[78] In analogy to FDET, in the SDFT approach, the charge of each subsystem is assumed to be an integer, whereas PDFT allows for fractional subsystem charges. In the exact limit, both SDFT and PDFT lead to the exact ground-state electronic density and energy of the total system under investigation, providing an alternative to the conventional supermolecular Kohn−Sham framework. This should be contrasted with the FDET approach, which does not target the exact ground-state electronic density of the total system AB but, rather, the density of subsystem A that minimizes the Hohenberg−Kohn energy functional of the total system, $E_{HK}[\rho_A + \rho_B]$, using a fixed form of the environment density ρ_B in the presence of constraints, as in eqs 6−9. Thus, FDET may lead to the same total ground-state density as SDFT, Kohn−Sham DFT, or PDFT, but only when the specific set of additional assumptions and constraints is employed.[48] Indeed, in the case of the total system AB consisting of two subsystems A and B, where A is a molecular system embedded in environment B, the SDFT approach searches for the pure-state, noninteracting, v-representable subsystem densities ρ_A and ρ_B that minimize the Hohenberg−Kohn energy functional $E_{HK}[\rho_A + \rho_B]$

$$E^{(AB)} = \min_{\rho_A,\rho_B} E_{HK}[\rho_A + \rho_B] \quad (14)$$

subject to the constraints given by eqs 6−9. Thus, the sufficient condition for reaching the exact ground-state density of the total system AB, ρ_{AB}, in SDFT is the decomposability of ρ_{AB} into a sum of two pure-state, noninteracting, v-representable densities ρ_A and ρ_B representing subsystems A and B consisting of the integer numbers of electrons, N_A and N_B, respectively (see the discussion in ref 48). The FDET approach does not search for the exact ground-state density ρ_{AB} of the total system AB. It uses the variational principle described by eq 7 to find the density, which minimizes the total ground-state energy in the presence of the constraint

$$\rho \geq \rho_B \quad (15)$$

with the subsystem density ρ_B given in advance. As a result, the total density obtained with FDET is not equal to the exact ground-state density ρ_{AB} except for one specific case where the difference between $\rho_{AB}(\vec{r})$ and the assumed density $\rho_B(\vec{r})$ is representable using one of the aforementioned auxiliary descriptors, including orbitals of the noninteracting reference system,[47] interacting wave function,[49] or one particle-density matrix.[50] Thus, by the virtue of the Hohenberg−Kohn theorem, unless

$\rho_B(\vec{r})$ is representable using the above auxiliary descriptors, the FDET approach can only give the upper bound to the exact ground-state energy of the total system *AB*,

$$E_{\mathrm{emb}}^{(A)}[\rho_B] \geq E^{(AB)} \tag{16}$$

Although there are differences between SDFT and FDET, as pointed out above, both methodologies have a lot in common as well. In particular, any computer implementation of the FDET approach can easily be converted into the SDFT algorithm. For example, as shown in the original numerical studies based on SDFT concerning atoms in solids[76,77] and in the recent implementation of SDFT for molecular liquids,[79] in the SDFT approach one has to solve a system of coupled Kohn−Sham equations, which is similar to the system represented by eq 13. One of the most efficient schemes for solving such systems is the "freeze-and-thaw" iterative procedure introduced in ref 80. The "freeze-and-thaw" algorithm was exploited in a number of SDFT studies, including those reported in refs 81−83, and the same algorithm is used in the present work to carry out the FDET calculations for the hydrogen-bonded complexes of the *cis*-7HQ system. The "freeze-and-thaw" scheme for solving the coupled Kohn−Sham-like equations of FDET and SDFT was previously used by us in the methodological studies on approximants to the bifunctional of the nonadditive kinetic energy potential $v_t^{\mathrm{nad}}[\rho_A,\rho_B](\vec{r})$ (see, e.g., refs 64, 84, and 85) and in the preparatory stages for the large-scale FDET simulations, in which the search defined by eq 7 is initially performed for smaller model systems in order to establish the adequacy of the simplified form of $\rho_B(\vec{r})$ to be used in the subsequent calculations for the target large system. We also demonstrated that the "freeze-and-thaw" procedure for solving the coupled Kohn−Sham-like equations of the type seen in eq 13 can be performed simultaneously with displacing nuclear positions, accelerating the SDFT-based geometry optimizations.[86]

Finally, it should be noted that the relaxation of the environment density ρ_B during the SDFT "freeze-and-thaw" iterations is accompanied by errors which are introduced by the approximant to the bifunctional of the nonadditive kinetic energy potential $v_t^{\mathrm{nad}}[\rho_A,\rho_B](\vec{r})$, eq 12, and which can artificially be enhanced by the relaxation of ρ_B. Thus, when the expected polarization effects are small, the relaxation of ρ_B during the SDFT iterations should be avoided, and the results presented in section 4 clearly show this. This problem does not enter the nonrelaxed FDET considerations, in which one fixes the form of ρ_B prior to FDET iterations. On the other hand, one needs to be aware of the fact that if the electronic polarization effects are strong or if the goal is to obtain embedding potentials that mimic supermolecular TDDFT calculations, one should use the fully relaxed "freeze-and-thaw" iterations to optimize both components of the total electronic density ρ_{AB}, i.e., ρ_A and ρ_B, not just ρ_A. Indeed, as shown in section 4, the FDET results for the spectral shifts in the *cis*-7HQ chromophore induced by complexation, in which ρ_B is allowed to relax, are quite close to the results of supermolecular TDDFT calculations, even though the latter results are generally poor and far from the EOMCC benchmark values and the corresponding experimental data. The fact that the relaxed FDET calculations lead to a considerably worse description of the complexation-induced shifts in *cis*-7HQ than the nonrelaxed ones has several reasons. One of them is the aforementioned problem of the errors introduced by the approximants used to represent $v_t^{\mathrm{nad}}[\rho_A,\rho_B](\vec{r})$, which penalize the overlap between ρ_A and ρ_B. Another is the realization of the fact that the relaxation of ρ_B in the FDET considerations is not necessarily the same as the physical effect of the electronic polarization of the environment *B* by subsystem *A*, i.e., one cannot expect automatic improvements in the results of the FDET calculations when ρ_B is allowed to relax, particularly when the polarization effects are small. The relaxation of the environment density ρ_B within the FDET framework is related to a complex notion of the pure-state noninteracting v-representability of the target subsystem density ρ_A, which does not automatically translate into the physical polarization of *B* by *A*. Indeed, let $\rho_{B,\mathrm{iso}}$ designate the exact ground-state density of the isolated species *B* and let $\rho_{B,\mathrm{fro}}$ be a particular choice of ρ_B used in FDET. If $\rho_{B,\mathrm{fro}}$ is chosen in such a way that the density difference $\overline{\rho}_A \equiv \rho_{AB} - \rho_{B,\mathrm{fro}}$, where ρ_{AB} represents the exact ground-state density of the total system *AB*, is pure-state v-representable, we can obtain this $\overline{\rho}_A$ by solving the Kohn−Sham system given by eq 13. Most likely, there is an infinite number of densities $\rho_{B,\mathrm{fro}}$ that lead to the pure-state v-representable $\overline{\rho}_A$. Each one of them will result in a different solution for $\overline{\rho}_A$ and, what is more important here, in a different relaxation, as measured by the difference $\Delta\rho_B \equiv \rho_{B,\mathrm{fro}} - \rho_{B,\mathrm{iso}}$. In particular, if $\rho_{B,\mathrm{iso}}$ is one of the densities $\rho_{B,\mathrm{fro}}$ that guarantees the pure-state noninteracting v-representability of $\overline{\rho}_A$, there is no physical relaxation at all ($\Delta\rho_B = 0$), and the "freeze-and-thaw" calculations are not needed, regardless of whether the physical polarization of *B* by *A* is significant or not. It is also worth mentioning that although the pure-state noninteracting v-representability of $\overline{\rho}_A$ cannot be *a priori* assured, there are strong indications from the recent studies of exactly solvable systems[54] that even if the *N*-representable density $\overline{\rho}_A$ associated with a given $\rho_{B,\mathrm{fro}}$ is not pure-state v-representable, it can be approached arbitrarily closely by a solution of eq 13 obtained with a suitably chosen smooth embedding potential. All of this demonstrates that the connection between the mathematical (in practice, numerical) relaxation of ρ_B in the FDET considerations and the physical polarization of the environment *B* by subsystem *A* is far from obvious. For this reason, comparing the results of the nonrelaxed and relaxed FDET calculations with the independent high-level *ab initio* data obtained with the carefully validated wave function theory is very important. The main objective of the present study is to demonstrate that when the polarization of the environment is small, as is the case when the weakly bound complexes of the *cis*-7HQ molecule are examined, one is better off by using a simplified FDET procedure in which the relaxation of the *a priori* determined environment density ρ_B is neglected, as this leads to a considerably better agreement with the results of the converged EOMCC calculations and the experiment.

2.2. Equation-of-Motion Coupled-Cluster Calculations. The main goal of the present work is to compare the shifts in the $\pi \rightarrow \pi^*$ excitation energy of the *cis*-7HQ system, induced by the complexation of *cis*-7HQ with small hydrogen bonded molecules, obtained with the FDET approach, with the results of the supermolecular EOMCC calculations with singles, doubles, and noniterative triples, exploiting the size-intensive modification of the CR-EOMCC(2,3) approach,[29,30] abbreviated as δ-CR-EOMCC(2,3), which is used to provide the required reference theoretical data. The basic idea of the EOMCC formalism is the following wave function ansatz:[6−9]

$$|\Psi_\mu\rangle = R_\mu \, \mathrm{e}^T |\Phi\rangle \tag{17}$$

where $|\Psi_\mu\rangle$ is the ground ($\mu = 0$) or excited ($\mu > 0$) state, $|\Phi\rangle$ is the reference determinant, which usually is the Hartree−Fock state [in all of the EOMCC calculations reported in this work, the restricted Hartree−Fock (RHF) configuration], and R_μ is the linear excitation operator which generates the excited-state wave functions $|\Psi_\mu\rangle$ from the CC ground state $|\Psi_0\rangle = e^T|\Phi\rangle$. Here and elsewhere in this article, we use a convention in which the $\mu = 0$ excitation operator $R_{\mu=0}$ is defined as a unit operator, $R_{\mu=0} = \mathbf{1}$, to incorporate the ground- and excited-state cases within a single set of formulas. The T operator entering the above definitions is the usual cluster operator of the ground-state CC theory, which is typically obtained by truncating the corresponding many-body expansion

$$T = \sum_{n=1}^{N} T_n \tag{18}$$

where

$$T_n = \sum_{i_1 < \ldots < i_n,\, a_1 < \ldots < a_n} t_{a_1 \ldots a_n}^{i_1 \ldots i_n} a^{a_1} \ldots a^{a_n} a_{i_n} \ldots a_{i_1} \tag{19}$$

is the n-body component of T, at some, preferably low, excitation level $M < N$, and by solving the nonlinear system of equations for cluster amplitudes $t_{a_1 \ldots a_n}^{i_1 \ldots i_n}$ with $n \leq M$, which define the truncated form of T, designated as $T^{(M)}$, resulting from the substitution of the CC wave function ansatz into the electronic Schrödinger equation and the projection of the resulting equation on the excited determinants $|\Phi_{i_1 \ldots i_n}^{a_1 \ldots a_n}\rangle$ that correspond to the many-body components T_n included in $T^{(M)}$. Here and elsewhere in the present article, we use a standard notation in which $i_1,i_2,\ldots$ or $i,j,\ldots$ and $a_1,a_2,\ldots$ or $a,b,\ldots$ are the occupied and unoccupied spin−orbitals, respectively, and a^{a_κ} (a_{i_κ}) designate the usual creation (annihilation) operators. Once the ground-state operator T and the corresponding ground-state CC energy E_0 are determined, one obtains the many-body components

$$R_{\mu,n} = \sum_{i_1 < \ldots < i_n,\, a_1 < \ldots < a_n} r_{\mu,\, a_1 \ldots a_n}^{i_1 \ldots i_n} a^{a_1} \ldots a^{a_n} a_{i_n} \ldots a_{i_1} \tag{20}$$

of the linear excitation operator

$$R_\mu = r_{\mu,0} 1 + \sum_{n=0}^{N} R_{\mu,n} \tag{21}$$

which is typically truncated at the same excitation level M as the cluster operator T, and the corresponding vertical excitation energies

$$\omega_\mu = E_\mu - E_0 \tag{22}$$

by solving the EOMCC eigenvalue problem involving the similarity-transformed Hamiltonian $\bar{H}^{(M)} = e^{-T^{(M)}} H e^{T^{(M)}}$ in the subspace of the N-electron Hilbert space spanned by the excited determinants $|\Phi_{i_1 \ldots i_n}^{a_1 \ldots a_n}\rangle$ that correspond to the many-body components $R_{\mu,n}$ included in R_μ.

The basic EOMCC approximation, in which $M = 2$, so that $T \approx T^{(2)} = T_1 + T_2$ and $R_\mu \approx R_\mu^{(2)} = r_{\mu,0}\mathbf{1} + R_{\mu,1} + R_{\mu,2}$, defining the EOMCCSD approach,[7−9] in which one diagonalizes the similarity-transformed Hamiltonian of CCSD, $\bar{H}^{(2)} = e^{-T^{(2)}} H e^{T^{(2)}}$, in the space spanned by singly and doubly excited determinants $|\Phi_i^a\rangle$ and $|\Phi_{ij}^{ab}\rangle$, and its linear-response CCSD counterpart[15,16] have been successful in describing excited states dominated by one-electron transitions, but this success does not automatically extend to the more complicated, more multireference excited electronic states, such as those characterized by a significant two-electron excitation nature (cf. refs 29, 30, 87−93 for examples). There also are cases of excited states dominated by singles, where the EOMCCSD theory level may be insufficient to obtain high-quality results.[94,95] Thus, particularly in the context of this study, where we expect the EOMCC theory to provide accurate reference data for the FDET and TDDFT calculations, it is important to examine if the EOMCC results used by us are reasonably well converged with the truncations in T and R_μ. Ideally, one would like to perform the full EOMCCSDT (EOMCC with singles, doubles, and triples) calculations[96−98] and compare them with the corresponding EOMCCSD results to see if the latter results are accurate enough. Unfortunately, it is virtually impossible to carry out the full EOMCCSDT calculations for the *cis*-7HQ system and its complexes investigated in this work due to a steep increase of the CPU time and storage requirements characterizing the EOMCCSDT approach that scale as $n_o^3 n_u^5$ and $\sim n_o^3 n_u^3$ with the numbers of occupied and unoccupied orbitals, n_o and n_u, respectively, as opposed to the $n_o^2 n_u^4$ CPU time and $\sim n_o^2 n_u^2$ storage requirements of EOMCCSD. Thus, one has to resort to one of the approximate treatments of triple excitations in EOMCC that replace the prohibitively expensive iterative CPU steps of EOMCCSDT that scale as $\mathcal{N}^8$ with the system size $\mathcal{N}$ to the more manageable $\mathcal{N}^6$−$\mathcal{N}^7$ steps.

A large number of approximate EOMCCSDT approaches and their linear-response analogs have been proposed to date.[29−32,87−89,91,92,96,97,99−106] The noniterative EOMCC methods, in which one adds corrections due to triples to the EOMCCSD energies, such as EOM-CC(2)PT(2)[100] and its size-intensive EOM-CCSD(2)$_T$[31] analog, CCSDR3,[102,103] EOMCCSD(T),[101] EOMCCSD($\tilde{T}$),[32] EOMCCSD(T′),[32] CR-EOMCCSD(T)[87,88,91,92] and the related N-EOMCCSD(T) approach,[106] and CR-EOMCC(2,3),[29,30] including the spin-flip variant of the CR-EOMCC(2,3) approach of refs 29 and 30 considered in ref 107, are particularly promising in this regard, since they represent computational black boxes similar to those of the popular CCSD(T) ground-state approach[108] or its CR-CC(2,3) extension.[26−28] All of the above methods greatly reduce the computer costs of full EOMCCSDT calculations, while improving the EOMCCSD results. The improvements are particularly significant for the excited states characterized by significant double-excitation components, but they are often non-negligible for states dominated by one-electron transitions. For example, the most promising EOM-CCSD(2)$_T$, CCSDR3, EOMCCSD($\tilde{T}$), CR-EOMCCSD(T), N-EOMCCSD(T), and CR-EOMCC(2,3) approaches are characterized by the iterative $n_o^2 n_u^4$ steps of EOMCCSD and the noniterative $n_o^3 n_u^4$ steps needed to construct the triples corrections to the EOMCCSD energies, while eliminating the need for storing the $\sim n_o^3 n_u^3$ triply excited amplitudes defining the T and R_μ operators. This makes these methods applicable to much larger problems than those that can be handled by full EOMCCSDT, including the hydrogen-bonded complexes of the *cis*-7HQ system considered in this work.

In this paper, we focus on the size-intensive modification of the CR-EOMCC(2,3) method of refs 29 and 30 defining the δ-CR-EOMCC(2,3) approach implemented in this work. The CR-EOMCC(2,3) approach and the underlying ground-state CR-CC(2,3) approximation[26−28] are examples of the renormalized CC/EOMCC schemes, which are based on the idea of adding the *a posteriori*, noniterative, and state-specific corrections

δ_μ due to higher-order excitations, neglected in the conventional CC/EOMCC calculations defined by some truncation level M, such as CCSD or EOMCCSD, to the corresponding CC/EOMCC energies. The formal basis for deriving the computationally manageable expressions for corrections δ_μ is provided by one of the forms[26,27,87−89,109−111] of the expansion describing the difference between the full CI and CC/EOMCC energies in terms of the generalized moments of the CC/EOMCC equations characterizing the truncated CC/EOMCC method we want to correct. If we are interested in correcting the results of the CC/EOMCC calculations truncated at M-tuple excitations, the moments that enter the expressions for the relevant energy corrections δ_μ are defined as projections of the CC/EOMCC equations with T and R_μ truncated at M-body components on the excited determinants $|\Phi^{a_1\ldots a_n}_{i_1\ldots i_n}\rangle$ with $n > M$ that are disregarded in the conventional CC/EOMCC considerations, i.e.

$$\mathscr{M}^{i_1\ldots i_n}_{\mu,a_1\ldots a_n}(M) = \langle \Phi^{a_1\ldots a_n}_{i_1\ldots i_n}|(\bar{H}^{(M)}R^{(M)}_\mu)|\Phi\rangle \qquad (23)$$

[$R^{(M)}_\mu$ in eq 23 is the R_μ operator truncated at the M-body component $R_{\mu,M}$]. All of the resulting moment expansions of the full CI energy of the μth electronic state can be cast into the generic form

$$\delta_\mu = \sum_{n=M+1}^{N_{\mu,M}} \sum_{i_1<\ldots<i_n,\, a_1<\ldots<a_n} \mathscr{l}^{a_1\ldots a_n}_{\mu,i_1\ldots i_n}\mathscr{M}^{i_1\ldots i_n}_{\mu,a_1\ldots a_n}(M) \qquad (24)$$

with $N_{\mu,M}$ representing the highest value of n for which $\mathscr{M}^{i_1\ldots i_n}_{\mu,a_1\ldots a_n}(M)$ is still nonzero, and the only essential difference between various approximations based on eq 24 is in the way one handles the coefficients $\mathscr{l}^{a_1\ldots a_n}_{\mu,i_1\ldots i_n}$.

In the specific case of the CR-EOMCC(2,3) approach that interests us here, one calculates the energies of the ground and excited states as

$$E_\mu = E^{(\mathrm{CCSD})}_\mu + \sum_{i<j<k,\, a<b<c} \mathscr{l}^{abc}_{\mu,ijk}\mathscr{M}^{ijk}_{\mu,abc}(2) \qquad (25)$$

where $E^{(\mathrm{CCSD})}_\mu$ are the CCSD ($\mu = 0$) and EOMCCSD ($\mu > 0$) energies, $\mathscr{M}^{ijk}_{\mu,abc}(2)$ are the moments of the CCSD/EOMCCSD equations corresponding to triple excitations, which are defined by eq 23 in which $M = 2$, and $\mathscr{l}^{abc}_{\mu,ijk}$ are the deexcitation amplitudes that one can calculate using the quasi-perturbative expressions shown in refs 29 and 30. The $\mathscr{l}^{abc}_{\mu,ijk}$ amplitudes used in the CR-EOMCC(2,3) considerations are expressed in terms of the one- and two-body components of the deexcitation operator defining the left EOMCCSD eigenstate,[9] and the one-body, two-body, and—in the full implementation of CR-EOMCC(2,3) defining variant D of it designated as CR-EOMCC(2,3),D—selected three-body components of the similarity-transformed Hamiltonian of CCSD, $\bar{H}^{(2)}$. The latter components enter the Epstein−Nesbet-like denominator for triples defining the $\mathscr{l}^{abc}_{\mu,ijk}$ amplitudes in the CR-EOMCC(2,3),D approach. In the simplified variant A of CR-EOMCC(2,3), abbreviated as CR-EOMCC(2,3),A and equivalent to the EOM-CC(2)PT(2) method of ref 100, one replaces the Epstein−Nesbet-like denominator defining $\mathscr{l}^{abc}_{\mu,ijk}$, which in variant D of CR-EOMCC(2,3) is calculated as $\omega^{(\mathrm{CCSD})}_\mu - (\langle\Phi^{abc}_{ijk}|\bar{H}^{(2)}_1|\Phi^{abc}_{ijk}\rangle + \langle\Phi^{abc}_{ijk}|\bar{H}^{(2)}_2|\Phi^{abc}_{ijk}\rangle + \langle\Phi^{abc}_{ijk}|\bar{H}^{(2)}_3|\Phi^{abc}_{ijk}\rangle)$, where $\omega^{(\mathrm{CCSD})}_\mu$ is the EOMCCSD excitation energy and $\bar{H}^{(2)}_n$ is the n-body component of $\bar{H}^{(2)}$, by the simplified form of it, which represents the Møller−Plesset-like denominator for triple excitations, $\omega^{(\mathrm{CCSD})}_\mu - (\varepsilon_a + \varepsilon_b + \varepsilon_c - \varepsilon_i - \varepsilon_j - \varepsilon_k)$. The differences between variants A and D are substantial, in favor of CR-EOMCC(2,3),D, when the excited states of interest are dominated by two-electron transitions. When the excited states in question are dominated by one-electron transitions, as is the case when we examine the $\pi \rightarrow \pi^*$ excitations in *cis*-7HQ and its complexes, the CR-EOMCC(2,3),A and CR-EOMCC(2,3),D approaches provide similar results. We refer the reader to the original work on the CR-EOMCC(2,3) approach and its variants[29,30] for further details. The similarity of the CR-EOMCC(2,3),A and CR-EOMCC(2,3),D excitation energies for the *cis*-7HQ system and its hydrogen-bonded complexes examined in this study is shown in section 4.1.

Before discussing the computational details of the FDET, TDDFT, and EOMCC calculations reported in this work, we must explain how one obtains the desired δ-CR-EOMCC(2,3) results. As shown in refs 30 and 31, although the ground-state CR-CC(2,3),D energy and its CR-CC(2,3),A analog, which is equivalent to the CCSD(2)$_\mathrm{T}$ approach of ref 112, are size extensive, being ideally suited for examining the weakly bound complexes involving larger molecules,[43−45] such as those studied in this work, their excited state CR-EOMCC(2,3),D and CR-EOMCC(2,3),A [or EOM-CC(2)PT(2)] analogs do not satisfy the property of size intensivity satisfied by EOMCCSD,[16,33] i.e., the vertical excitation energy of a noninteracting system $A + B$, in which fragment A is excited, resulting from the CR-EOMCC(2,3) or EOM-CC(2)PT(2) calculations, is not the same as that obtained for the isolated system A. Although the departure from strict size intensivity in the CR-EOMCC calculations of vertical and adiabatic excitation energies is in many cases of relatively minor significance when compared to other sources of errors,[92] this may be a more serious issue when examining the shifts in the excitation energy due to the formation of weakly bound complexes. The lack of size intensivity of the CR-EOMCC(2,3) and EOM-CC(2)PT(2) excitation energies can be traced back to the presence of the size-extensive contribution

$$\beta_\mu = \sum_{i<j<k,\, a<b<c} (r_{\mu,0}\mathscr{l}^{abc}_{\mu,ijk} - \mathscr{l}^{abc}_{0,ijk})\mathscr{M}^{ijk}_{0,abc}(2) \qquad (26)$$

in the vertical excitation energy

$$\omega^{(\text{CR-EOMCC}(2,3))}_\mu = E^{(\text{CR-EOMCC}(2,3))}_\mu - E^{(\text{CR-CC}(2,3))}_0 \qquad (27)$$

Indeed, using the above equations for the CR-EOMCC(2,3) energies, particularly eq 25, we can decompose the CR-EOMCC(2,3) excitation energy as follows:[30,31]

$$\omega^{(\text{CR-EOMCC}(2,3))}_\mu = \omega^{(\mathrm{CCSD})}_\mu + \alpha_\mu + \beta_\mu \qquad (28)$$

Here, $\omega^{(\mathrm{CCSD})}_\mu$ is the vertical excitation energy of EOMCCSD,

$$\alpha_\mu = \sum_{i<j<k,\, a<b<c} \mathscr{l}^{abc}_{\mu,ijk}\tilde{\mathscr{M}}^{ijk}_{\mu,abc}(2) \qquad (29)$$

where $\tilde{\mathscr{M}}^{ijk}_{\mu,abc}(2) = \langle\Phi^{abc}_{ijk}|\bar{H}^{(2)}(R_{\mu,1} + R_{\mu,2})|\Phi\rangle$ is the contribution to the triply excited moment $\mathscr{M}^{ijk}_{\mu,abc}(2)$ of EOMCCSD due to the one- and two-body components of $R^{(2)}_\mu$, and β_μ is the quantity defined by eq 26. Since the EOMCCSD approach is rigorously size intensive and, as shown in ref 31, the α_μ term is size intensive as well, the $[\omega^{(\mathrm{CCSD})}_\mu + \alpha_\mu(2,3)]$ part of the

CR-EOMCC(2,3) excitation energy $\omega_\mu^{(\text{CR-EOMCC(2,3)})}$ is a size-intensive quantity. Unfortunately, the β_μ term defined by eq 26, being a size-extensive contribution that does not cancel out, grows with the size of the system,[30,31] destroying the size intensivity of $\omega_\mu^{(\text{CR-EOMCC(2,3)})}$. In order to address this concern and following the discussion in refs 30 and 31 in this work, we have implemented the rigorously size-intensive variant of CR-EOMCC(2,3), designated as δ-CR-EOMCC(2,3), by neglecting the problematic β_μ term in eq 28 and redefining the excitation energy as follows:

$$\omega_\mu^{(\delta\text{-CR-EOMCC(2,3)})} = \omega_\mu^{(\text{CCSD})} + \alpha_\mu \tag{30}$$

with α_μ given by eq 29. The resulting δ-CR-EOMCC(2,3) approach provides a size-intensive description of the excitation energies and, by defining the total energy of a given electronic state μ, i.e., E_μ, as a sum of the size-extensive ground-state CR-CC(2,3) energy and size-intensive excitation energy $\omega_\mu^{(\delta\text{-CR-EOMCC(2,3)})}$, eq 30, so that

$$\begin{aligned} E_\mu &= E_0^{(\text{CR-CC(2,3)})} + \omega_\mu^{(\delta\text{-CR-EOMCC(2,3)})} \\ &= E_\mu^{(\text{CCSD})} + \sum_{i<j<k,\, a<b<c} \mathcal{l}_{0,ijk}^{abc} \mathscr{M}_{0,abc}^{ijk}(2) \\ &\quad + \sum_{i<j<k,\, a<b<c} \mathcal{l}_{\mu,ijk}^{abc} \tilde{\mathscr{M}}_{\mu,abc}^{ijk}(2) \end{aligned} \tag{31}$$

the size extensive description of state μ, assuming that the electronic excitation in AB is either in A or in B, but not in both fragments simultaneously (cf. refs 16, 33, and 92). Again, as in the regular CR-EOMCC(2,3) approach, we can distinguish between the full variant D of $\omega_\mu^{(\delta\text{-CR-EOMCC(2,3)})}$ and its various approximations, including variant A. The δ-CR-EOMCC(2,3),A method is equivalent to the EOMCCSD(2)$_T$ approach of ref 31 and, if we limit ourselves to the vertical excitation energies only, to the EOMCCSD($\tilde{\text{T}}$) approach of ref 32. As shown in section 4.1, variants A and D provide nearly identical results for the vertical excitation energies in the *cis*-7HQ chromophore and its complexes, corresponding to the lowest $\pi \rightarrow \pi^*$ transition, which seem to be in good agreement with the experimental data reported in refs 5 and 59.

3. COMPUTATIONAL DETAILS

In order to examine the performance of the FDET approach and to demonstrate its advantages when compared with the results of supermolecular TDDFT calculations, both benchmarked against the high-level EOMCC data of δ-CR-EOMCC(2,3) quality, we have investigated the shifts in the vertical excitation energy $\omega_{\pi\rightarrow\pi^*}$ corresponding to the lowest $\pi \rightarrow \pi^*$ transition in the *cis*-7HQ chromophore induced by the formation of hydrogen-bonded complexes shown in Figure 1, which were previously examined using laser resonant two-photon UV spectroscopy.[5,59] The eight complexes considered in this work include the *cis*-7HQ···B systems, where B represents one of the following environments: a single water molecule, a single ammonia molecule, a water dimer, a single molecule of methanol, a single molecule of formic acid, a trimer consisting of ammonia and two water molecules, a trimer consisting of ammonia, water, and ammonia, and a trimer consisting of two ammonia and one water molecules (see Figure 1). For each *cis*-7HQ···B complex and for each electronic structure approach employed in this study, the corresponding environment-induced shift $\Delta\omega_{\pi\rightarrow\pi^*}$ was calculated as a difference between the value of $\omega_{\pi\rightarrow\pi^*}$ characterizing the complex and that obtained for the isolated *cis*-7HQ molecule, using the nuclear geometries of *cis*-7HQ···B and *cis*-7HQ optimized in the second-order Møller−Plesset perturbation theory (MP2)[113] calculations employing the aug-cc-pVTZ basis set.[114,115] The optimizations of nuclear geometries of the *cis*-7HQ and *cis*-7HQ···B systems were performed using the analytic gradients of MP2 available in the Gaussian 03 package.[116] As in all other post-Hartree−Fock wave function calculations discussed in this article, the lowest-energy core molecular orbitals (MOs) correlating with the 1s shells of the C, N, and O atoms were frozen in these optimizations.

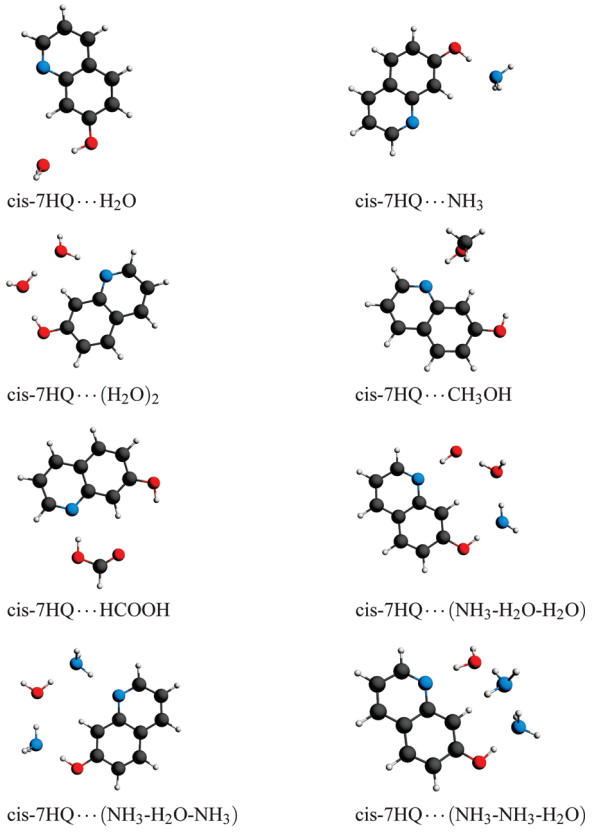

Figure 1. The eight hydrogen-bonded complexes of the *cis*-7HQ molecule studied in the present work.

Once the nuclear geometries of the *cis*-7HQ and *cis*-7HQ···B systems were determined, we performed the desired FDET and supermolecular TDDFT and EOMCC calculations of the vertical excitation energies $\Delta\omega_{\pi\rightarrow\pi^*}$ and the environment-induced shifts $\Delta\omega_{\pi\rightarrow\pi^*}$. The most essential information about these calculations, including basis sets, key algorithmic details, and computer codes used to perform them, is provided below.

3.1. Reference EOMCC Calculations. In order to establish the reference EOMCC values of the environment-induced shifts $\Delta\omega_{\pi\rightarrow\pi^*}$, we performed a series of EOMCCSD calculations for the *cis*-7HQ, 7HQ···H_2O, and 7HQ···NH_3 systems using five different basis sets, including 6-31+G(d),[117−119] 6-31++G(d,p),[117−119] 6-311+G(d),[119,120] aug-cc-pVDZ,[114,115] and the [5s3p2d/3s2p] basis of Sadlej,[121] designated as POL, followed by the EOMCCSD and δ-CR-EOMCC(2,3) computations for all eight *cis*-7HQ···B complexes examined in this work using the largest basis sets that we could afford, namely,

6-311+G(d) in the EOMCCSD case and 6-31+G(d) in the case of the δ-CR-EOMCC(2,3) approach. The main purpose of all of these calculations was to examine the stability of the final EOMCC values of the $\Delta\omega_{\pi\rightarrow\pi^*}$ shifts, recommended for use in benchmarking the FDET and supermolecular TDDFT data, with respect to the choice of the basis set and higher-order correlation effects neglected in EOMCCSD, but included in δ-CR-EOMCC(2,3). As explained in section 4.1, the final EOMCC values of the vertical excitation energies $\omega_{\pi\rightarrow\pi^*}$ that are used in this paper to benchmark the FDET and supermolecular TDDFT methods were obtained using the composite approach, in which we augment the EOMCCSD/6-311+G(d) results by the triples corrections to EOMCCSD energies extracted from the δ-CR-EOMCC(2,3)/6-31+G(d) calculations, as in the following formula:

$$\begin{aligned}\omega_{\pi\rightarrow\pi^*}(\mathrm{EOMCC}) &= \omega_{\pi\rightarrow\pi^*}(\mathrm{EOMCCSD/6\text{-}311+G(d)}) \\ &+ [\omega_{\pi\rightarrow\pi^*}(\delta\text{-CR-EOMCC(2,3)/6-31+G(d)}) \\ &- \omega_{\pi\rightarrow\pi^*}(\mathrm{EOMCCSD/6\text{-}31+G(d)})] \quad (32)\end{aligned}$$

All of the EOMCC calculations reported in this work were carried out with the programs developed at Michigan State University described, for example, in refs 26, 30, 91, and 92, that form part of the GAMESS package.[122,123] In order to obtain the final δ-CR-EOMCC(2,3) results, we had to modify the previously developed[26,30] CR-CC(2,3)/CR-EOMCC(2,3) GAMESS routines, since we had to replace the vertical excitation energy of CR-EOMCC(2,3) given by eq 28 with its size-intensive δ-CR-EOMCC(2,3) counterpart defined by eq 30. Thanks to this effort, the present GAMESS code enables the calculations of three different types of triples corrections to EOMCCSD energies, including CR-EOMCCSD(T),[87,88,91,92] CR-EOMCC(2,3),[29,30] and δ-CR-EOMCC(2,3), as defined by eqs 30 and 31. The corresponding ground-state CCSD calculations, which precede the determination of the left CCSD and right and left EOMCCSD eigenstates that enter the formulas for the triples corrections of δ-CR-EOMCC(2,3) and the steps needed to compute the triples corrections of the ground-state CR-CC(2,3) and excited-state CR-EOMCC(2,3) and δ-CR-EOMCC(2,3) approaches, were performed with the routines described in ref 124, which form part of GAMESS as well. The RHF orbitals were employed throughout, and as pointed out above, the lowest-energy core MOs that correlate with the 1s shells of the non-hydrogen atoms were frozen in the CCSD, EOMCCSD, and δ-CR-EOMCC(2,3) calculations. The CCSD/EOMCCSD energies were converged to 10^{-7} Hartree. We refer the reader to refs 26, 30, 91, and 92 for further details of the EOMCC computer codes and algorithms exploited in this work.

3.2. FDET and Supermolecular TDDFT Calculations. All of the FDET and supermolecular TDDFT calculations reported in this article were performed using the linear-response TDDFT routines available in the ADF2009.01 code.[125] In particular, the FDET calculations followed the general protocol introduced in ref 58 in which the occupied and unoccupied orbitals for the embedded chromophore that are obtained by solving the Kohn–Sham-like system defined by eq 13 are subsequently used within the linear-response TDDFT framework[46] to obtain excitation energies.

In order to examine the effect of the basis set on the complexation-induced shifts $\Delta\omega_{\pi\rightarrow\pi^*}$, three STO-type basis sets[125] were employed in the FDET and supermolecular TDDFT calculations: STO DZP (double-ζ basis with one set of polarization functions), STO TZ2P (triple-ζ basis with two sets of polarization functions), and STO ATZ2P, which includes all TZ2P functions plus one set of diffuse s-STO and p-STO functions.

The environment density ρ_B used in the FDET calculations was either nonrelaxed, i.e., constructed using the ground-state electronic density of the environment obtained by solving the conventional Kohn–Sham equations for the environment molecules in the absence of the chromophore, or relaxed, i.e., obtained with the aforementioned "freeze-and-thaw" procedure.[80] We also examined two types of basis expansions to represent the occupied and unoccupied orbitals of the chromophore A embedded in the environment B and densities ρ_A and ρ_B in the FDET calculations. In the supermolecular expansion approach, all atomic centers of the total system AB were used to represent the orbitals and densities. In the monomer-expansion FDET calculations, the orbitals of the chromophore A embedded in B and the corresponding density ρ_A were represented using the atomic centers of A, whereas the environment density ρ_B was represented using the atomic centers of B (see refs 80 and 126 for further information). The monomer-expansion technique using nonrelaxed ρ_B, which is the recommended variant of FDET for the type of applications reported in this article, relies on the approximation, referred to as the Neglect of Dynamic Response of the Environment (NDRE), in which we assume that the dynamic response of the whole system AB to the process of electronic excitation is limited to chromophore A and that the coupling between the excitations in the embedded system and in its environment can be neglected. A comparison of the complexation-induced shifts $\Delta\omega_{\pi\rightarrow\pi^*}$ in the *cis*-7HQ$\cdots B$ systems resulting from the FDET and EOMCC calculations, discussed in the next section, clearly shows that such coupling can indeed be neglected, as the spectral overlap between *cis*-7HQ and the environment molecules bound to it is negligible. The NDRE approximation and the monomer-expansion-based FDET approach that results from it are very effective in eliminating spurious electronic excitations involving the environment (see the discussion in ref 52). If the coupling between the excitations in the embedded system and in its environment could not be neglected, we would have to rely on the more general formalism introduced in ref 127 (for the additional discussion of the importance of such couplings in FDET calculations, see ref 128).

In both the FDET and supermolecular TDDFT calculations, we used the SAOP scheme[129] to approximate the relevant exchange-correlation potential contributions for the isolated and embedded chromophore (the FDET case) and for the total system (the supermolecular TDDFT case). The nonadditive kinetic energy potential $v_t^{\mathrm{nad}}[\rho_A,\rho_B](\vec{r})$, eq 12, that forms part of the local, orbital-free embedding potential $v_{\mathrm{emb}}^{\mathrm{eff}}[\rho_A,\rho_B;\vec{r}]$, eq 10, used in the FDET calculations was approximated using the generalized gradient approximation (GGA97),[126] whereas the nonadditive exchange-correlation component of $v_{\mathrm{emb}}^{\mathrm{eff}}[\rho_A,\rho_B;\vec{r}]$, eq 11, was approximated using the Perdew–Wang (PW91) functional. We also performed calculations in which the nonadditive kinetic energy potential $v_t^{\mathrm{nad}}[\rho_A,\rho_B](\vec{r})$ was approximated with the help of the recently developed NDSD approximant,[64] which takes into account the exact conditions that become relevant for the proper behavior of $v_t^{\mathrm{nad}}[\rho_A,\rho_B](\vec{r})$ in the vicinity of nuclei, but we do not show these results in this article, since they are very similar to those obtained with GGA97. Because of the small energy differences that define the spectral shifts examined in this work, we used

Table 1. Basis-Set Dependence of the Vertical Excitation Energies $\omega_{\pi\rightarrow\pi^*}$ and the Environment-Induced Shifts $\Delta\omega_{\pi\rightarrow\pi^*}$ (in cm^{-1}) Obtained with the EOMCCSD Approach Corresponding to the Lowest $\pi\rightarrow\pi^*$ Transition in the *cis*-7HQ Chromophore and Its Complexes with the Water and Ammonia Molecules

	$\omega_{\pi\rightarrow\pi^*}$			$\Delta\omega_{\pi\rightarrow\pi^*}$	
basis set	7HQ	7HQ···H_2O	7HQ···NH_3	7HQ···H_2O	7HQ···NH_3
6-31+G(d)	35171	34643	34396	−528	−775
6-31++G(d,p)	35120	34597	34351	−523	−769
6-311+G(d)	35046	34500	34263	−546	−783
aug-cc-pVDZ	34707	34182	33923	−525	−784
POL	34596	34077	33819	−519	−777

Table 2. Vertical Excitation Energies $\omega_{\pi\rightarrow\pi^*}$ and the Environment-Induced Shifts $\Delta\omega_{\pi\rightarrow\pi^*}$ (in cm^{-1}) Obtained with the EOMCCSD/6-31+G(d), EOMCCSD/6-311+G(d), δ-CR-EOMCC(2,3),A/6-31+G(d), and δ-CR-EOMCC(2,3),D/6-31+G(d) Approaches, and Their Composite EOMCC,A and EOMCC,D Analogs Defined by eq 32, Corresponding to the Lowest $\pi\rightarrow\pi^*$ Transition in the *cis*-7HQ Chromophore and Its Various Complexes

environment	EOMCCSD/ 6-31+G(d)	EOMCCSD/ 6-311+G(d)	δ-CR-EOMCC(2,3),A/ 6-31+G(d)	δ-CR-EOMCC(2,3),D/ 6-31+G(d)	EOMCC,A[a]	EOMCC,D[b]	Exp.[c]
			$\omega_{\pi\rightarrow\pi^*}$				
none	35171	35046	31103	30711	30977	30586	30830
H_2O	34643	34500	30558	30199	30415	30056	30240
NH_3	34396	34263	30291	29922	30157	29788	29925
$2H_2O$	33867	33699	29700	29378	29532	29210	29193
CH_3OH	34830	34695	30717	30428	30582	30293	30363
HCOOH	34505	34371	30368	30056	30235	29922	29816
$NH_3-H_2O-H_2O$	33381	33218	29171	28863	29008	28701	28340
$NH_3-H_2O-NH_3$	33542	33385	29355	29036	29197	28879	28694
$NH_3-NH_3-H_2O$	33302	33136	29088	28812	28922	28646	28348
			$\Delta\omega_{\pi\rightarrow\pi^*}$				
H_2O	−528	−546	−544	−512	−562	−530	−590
NH_3	−775	−783	−812	−789	−820	−797	−905
$2H_2O$	−1304	−1347	−1403	−1333	−1446	−1376	−1637
CH_3OH	−341	−351	−386	−283	−396	−292	−467
HCOOH	−666	−675	−734	−655	−743	−664	−1014
$NH_3-H_2O-H_2O$	−1790	−1828	−1932	−1847	−1969	−1885	−2490
$NH_3-H_2O-NH_3$	−1629	−1661	−1748	−1675	−1780	−1707	−2136
$NH_3-NH_3-H_2O$	−1869	−1910	−2014	−1899	−2055	−1940	−2482

[a] Defined by eq 32, in which variant A of CR-EOMCC(2,3) is employed. [b] Defined by eq 32, in which variant D of CR-EOMCC(2,3) is employed. [c] Obtained with laser resonant two-photon ionization UV spectroscopy.[5]

tight convergence criteria when solving the Kohn−Sham and linear-response TDDFT equations (10^{-10} hartree).

4. RESULTS AND DISCUSSION

The results of our FDET, supermolecular TDDFT, and EOMCC calculations for the shifts in the vertical excitation energy $\omega_{\pi\rightarrow\pi^*}$ corresponding to the lowest $\pi\rightarrow\pi^*$ transition in the *cis*-7HQ chromophore induced by the formation of the eight complexes shown in Figure 1 are summarized in Tables 1−8 and Figures 2−5. We begin our discussion with the analysis of the EOMCCSD and δ-CR-EOMCC(2,3) calculations aimed at establishing the reference EOMCC values for benchmarking purposes. The comparison of the FDET shifts $\Delta\omega_{\pi\rightarrow\pi^*}$ with the reference EOMCC, supermolecular TDDFT, and experimental data is presented immediately afterward. Among the key discussed aspects are the basis set dependence of the FDET and supermolecular TDDFT results, the issues created by relaxing the environment density ρ_B in the FDET calculations, the usefulness of the monomer vs supermolecular basis expansions in the FDET considerations, and the effect of the approximations that are used for the exchange-correlation potentials on the FDET and supermolecular TDDFT results.

4.1. Reference EOMCC Results. In order to establish the level of EOMCC theory that would be appropriate for serving as a reference for the FDET and supermolecular TDDFT calculations reported in this work, we first examine the dependence of the environment-induced shifts $\Delta\omega_{\pi\rightarrow\pi^*}$ resulting from the EOMCCSD calculations on the basis set. In Table 1, we compare the results of the EOMCCSD calculations obtained with the

Table 3. Comparison of the Environment-Induced Shifts $\Delta\omega_{\pi\rightarrow\pi^*}$ (in cm^{-1}) of the Vertical Excitation Energy Corresponding to the Lowest $\pi \rightarrow \pi^*$ Transition in the *cis*-7HQ Chromophore Resulting from the Monomer-Expansion-Based FDET and Supermolecular TDDFT Calculations Using the STO ATZ2P Basis Set with the Reference EOMCC,A Data

	supermolecular		FDET	
			nonrelaxed	relaxed
environment	EOMCC,A	TDDFT	ρ_B	ρ_B
H_2O	−562	−944	−645	−768
NH_3	−820	−1222	−816	−1005
$2H_2O$	−1446	−2280	−1624	−1975
CH_3OH	−396	−805	−454	−625
HCOOH	−743	−1569	−972	−1312
$NH_3-H_2O-H_2O$	−1969	−2838	−1863	−2342
$NH_3-H_2O-NH_3$	−1780	−2594	−1791	−2232
$NH_3-NH_3-H_2O$	−2055	−2899	−1890	−2436
av. dev. from EOMCC,A	0	−673	−36	−366
av. abs. dev. from EOMCC,A	0	673	104	366

Table 4. Environment-Induced Shifts $\Delta\omega_{\pi\rightarrow\pi^*}$ (in cm^{-1}) of the Vertical Excitation Energy Corresponding to the Lowest $\pi \rightarrow \pi^*$ Transition in the *cis*-7HQ Chromophore Resulting from the Supermolecular-Expansion-Based FDET and Supermolecular TDDFT Calculations Using the STO ATZ2P Basis Set, along with the Average Errors Relative to the Reference EOMCC,A Data

	supermolecular	FDET	
environment	TDDFT	nonrelaxed ρ_B	relaxed ρ_B
H_2O	−944	−529	−840
NH_3	−1222	−849	−1082
$2H_2O$	−2280	−1659	−2032
CH_3OH	−805	−474	−698
HCOOH	−1569	−1025	−1587
$NH_3-H_2O-H_2O$	−2838	−1933	−2526
$NH_3-H_2O-NH_3$	−2594	−1859	−2372
$NH_3-NH_3-H_2O$	−2899	−1940	−2524
av. dev. from EOMCC,A	−673	−62	−486
av. abs. dev. from EOMCC,A	673	108	486

Table 5. Environment-Induced Shifts $\Delta\omega_{\pi\rightarrow\pi^*}$ (in cm^{-1}) of the Vertical Excitation Energy Corresponding to the Lowest $\pi \rightarrow \pi^*$ Transition in the cis-7HQ Chromophore Resulting from the Monomer-Expansion-Based FDET and Supermolecular TDDFT Calculations Using the STO TZ2P Basis Set, along with the Average Errors Relative to the Reference EOMCC,A Data

	supermolecular	FDET	
environment	TDDFT	nonrelaxed ρ_B	relaxed ρ_B
H_2O	−876	−636	−757
NH_3	−1227	−849	−1016
$2H_2O$	−2298	−1635	−1962
CH_3OH	−847	−491	−665
HCOOH	−1602	−1012	−1334
$NH_3-H_2O-H_2O$	−2811	−1911	−2355
$NH_3-H_2O-NH_3$	−2519	−1806	−2177
$NH_3-NH_3-H_2O$	−2871	−1896	−2370
av. dev. from EOMCC,A	−660	−58	−358
av. abs. dev. from EOMCC,A	660	113	358

Table 6. Environment-Induced Shifts $\Delta\omega_{\pi\rightarrow\pi^*}$ (in cm^{-1}) of the Vertical Excitation Energy Corresponding to the Lowest $\pi \rightarrow \pi^*$ Transition in the *cis*-7HQ Chromophore Resulting from the Monomer-Expansion-Based FDET and Supermolecular TDDFT Calculations Using the STO DZP Basis Set, along with the Average Errors Relative to the Reference EOMCC,A Data

	supermolecular	FDET	
environment	TDDFT	nonrelaxed ρ_B	relaxed ρ_B
H_2O	−884	−641	−764
NH_3	−1220	−832	−1014
$2H_2O$	−2324	−1653	−1956
CH_3OH	−884	−525	−678
HCOOH	−1644	−1027	−1321
$NH_3-H_2O-H_2O$	−2862	−1925	−2364
$NH_3-H_2O-NH_3$	−2546	−1787	−2160
$NH_3-NH_3-H_2O$	−2886	−1896	−2353
av. dev. from EOMCC,A	−685	−64	−355
av. abs. dev. from EOMCC,A	685	115	355

6-31+G(d), 6-31++G(d,p), 6-311+G(d), aug-cc-pVDZ, and POL basis sets for the two smallest complexes, 7HQ···H_2O and 7HQ···NH_3, for which we could afford the largest number of computations. The results in Table 1 indicate that although the vertical excitation energies $\omega_{\pi\rightarrow\pi^*}$ in the bare *cis*-7HQ system and its complexes with the water and ammonia molecules vary with the basis set (for the basis sets tested here by as much as about 600 cm^{-1}), the environment-induced shifts $\Delta\omega_{\pi\rightarrow\pi^*}$ are almost insensitive to the basis set choice. Although we were unable to perform a similarly thorough analysis for the remaining complexes due to prohibitive computer costs, we were able to obtain the EOMCCSD $\omega_{\pi\rightarrow\pi^*}$ and $\Delta\omega_{\pi\rightarrow\pi^*}$ values for all of the complexes examined in this study using the 6-31+G(d) and 6-311+G(d) basis sets. As shown in Table 2, the differences between the EOMCCSD/6-31+G(d) and EOMCCSD/6-311+G(d) values of the environment-induced shifts $\Delta\omega_{\pi\rightarrow\pi^*}$ remain small for all complexes of interest, ranging from 8 cm^{-1} in the 7HQ···NH_3 case to 43 cm^{-1} in the case of 7HQ···$(H_2O)_2$, or 1−3%. Thus, we can conclude that the choice of the basis set, although important for obtaining the converged $\omega_{\pi\rightarrow\pi^*}$ values, is of relatively little significance when the environment-induced shifts in the vertical excitation energy corresponding to the lowest $\pi \rightarrow \pi^*$ transition in the *cis*-7HQ chromophore are considered.

Although the EOMCCSD approach is known to provide an accurate description of excited states dominated by one-electron transitions, such as the $\pi \rightarrow \pi^*$ transition in *cis*-7HQ and its complexes, there have been cases of similar states reported in the literature, where the EOMCCSD level has not been sufficient to obtain high-quality results.[94,95] Moreover, our interest in this study is in the small energy differences defining the

Table 7. Dependence of the Vertical Excitation Energy Corresponding to the Lowest $\pi \rightarrow \pi^*$ Transition in *cis*-7HQ Resulting from the Supermolecular TDDFT Calculations Using the STO TZ2P Basis Set (in cm^{-1}) on the Position of Ghost Functions

position of ghost functions	excitation energy
none	30494
H_2O	30470
NH_3	30503
$2H_2O$	30536
CH_3OH	30478
HCOOH	30500
$(NH_3-H_2O-H_2O)$	30468
$(NH_3-H_2O-NH_3)$	30516
$(NH_3-NH_3-H_2O)$	30454

Table 8. Effect of the Approximation Used for the Exchange-Correlation Energy Functional on the Environment-Induced Shifts $\Delta\omega_{\pi\rightarrow\pi^*}$ (in cm^{-1}) of the Vertical Excitation Energy Corresponding to the Lowest $\pi \rightarrow \pi^*$ Transition in the *cis*-7HQ Chromophore Calculated Using the FDET and Supermolecular TDDFT Methodologies and the STO ATZ2P Basis Set

	FDET[a]			supermolecular		
environment	PW91[b]	LDA[c]	SAOP[d]	PW91[b]	LDA[c]	SAOP[d]
H_2O	−724	−718	−645	−1031	−1014	−944
NH_3	−933	−922	−816	−1415	−1405	−1222
$2H_2O$	−1767	−1756	−1624	−2440	−2480	−2280
CH_3OH	−465	−461	−454	−856	−895	−805
HCOOH	−1007	−998	−972	−1578	−1611	−1569
$NH_3-H_2O-H_2O$	−2030	−2017	−1863	−3143	−3162	−2838
$NH_3-H_2O-NH_3$	−1975	−1960	−1791	−2899	−2930	−2594
$NH_3-NH_3-H_2O$	−2065	−2050	−1890	−3145	−3204	−2899
av. dev. from EOMCC,A	−149	−139	−36	−842	−866	−673
av. abs. dev. from EOMCC,A	149	140	104	842	866	673

[a] In FDET calculations, PW91, LDA, and SAOP refer to three different approximations for the exchange-correlation potential evaluated at the chromophore density ρ_A. The nonadditive contributions to the orbital-free embedding potential use the same approximants in all cases (PW91 for exchange-correlation and GGA97 for the kinetic energy). The FDET calculations use the nonrelaxed environment density ρ_B and the monomer basis expansion. [b] Ref 136. [c] Ref 135. [d] Ref 129.

environment-induced shifts $\Delta\omega_{\pi\rightarrow\pi^*}$, which may be sensitive to the higher-order correlation effects neglected in the EOMCCSD calculations. For this reason, we also examined the effect of triples corrections to EOMCCSD energies on the calculated $\omega_{\pi\rightarrow\pi^*}$ and $\Delta\omega_{\pi\rightarrow\pi^*}$ values by performing the δ-CR-EOMCC(2,3) calculations with the 6-31+G(d) basis set. The results of these calculations, shown in Table 2, indicate that triple excitations have a significant effect on the vertical excitation energies $\omega_{\pi\rightarrow\pi^*}$, reducing the 4000−5000 cm^{-1} differences between the EOMCCSD and experimental data to no more than about 800 cm^{-1}, when the δ-CR-EOMCC(2,3),A/6-31+G(d)

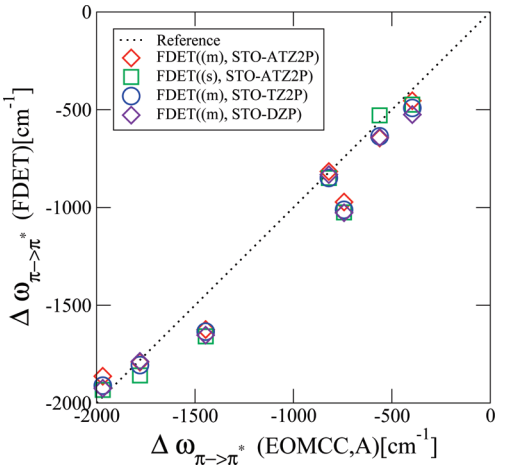

Figure 2. The dependence of the environment-induced shifts $\Delta\omega_{\pi\rightarrow\pi^*}$ of the vertical excitation energy corresponding to the lowest $\pi \rightarrow \pi^*$ transition in the *cis*-7HQ chromophore on the STO-type basis set used in the FDET calculations employing the monomer (m) and supermolecular (s) expansions and nonrelaxed ρ_B, and a comparison of the resulting FDET shifts with the reference EOMCC,A data.

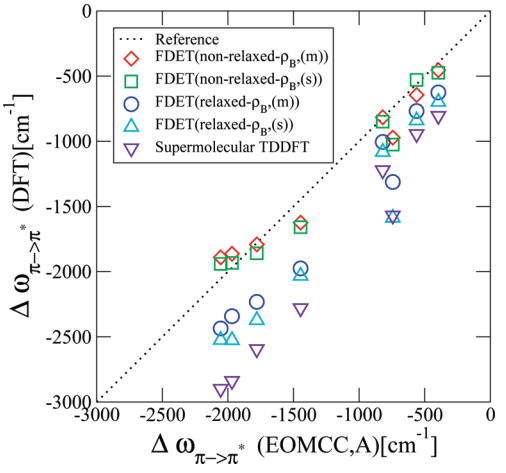

Figure 3. The dependence of the environment-induced shifts $\Delta\omega_{\pi\rightarrow\pi^*}$ of the vertical excitation energy corresponding to the lowest $\pi \rightarrow \pi^*$ transition in the *cis*-7HQ chromophore on the type of the frozen electron density ρ_B used in the FDET calculations employing the STO ATZ2P basis set and the monomer (m) and supermolecular (s) expansions, and a comparison of the resulting shifts with the reference EOMCC,A and supermolecular TDDFT data.

calculations are performed, and no more than about 500 cm^{-1} when the δ-CR-EOMCC(2,3),D/6-31+G(d) approach is employed, while bringing the $\Delta\omega_{\pi\rightarrow\pi^*}$ values closer to the experimentally observed shifts when compared with EOMCCSD. Although the differences between the δ-CR-EOMCC(2,3) and EOMCCSD values of the environment-induced shifts $\Delta\omega_{\pi\rightarrow\pi^*}$ resulting from the calculations with the 6-31+G(d) basis set do not exceed 15−16% of the EOMCCSD values, triples corrections improve the EOMCCSD results and, as such, are useful for the generation of the reference EOMCC data.

Ideally, one would like to perform the δ-CR-EOMCC(2,3) calculations for basis sets larger than 6-31+G(d), such as 6-311+G(d), but complexes of *cis*-7HQ examined in this study

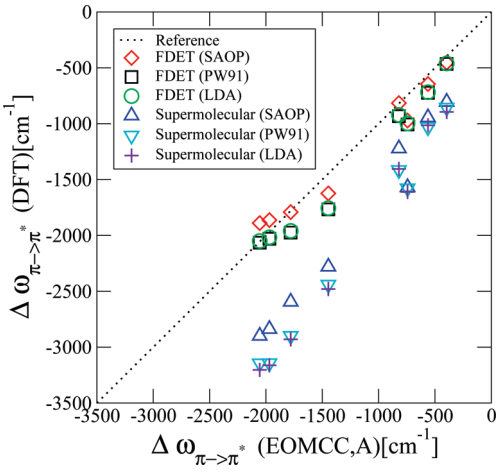

Figure 4. The dependence of the environment-induced shifts $\Delta\omega_{\pi\rightarrow\pi^*}$ of the vertical excitation energy corresponding to the lowest $\pi \rightarrow \pi^*$ transition in the *cis*-7HQ chromophore and resulting from the FDET and supermolecular TDDFT calculations with the STO ATZ2P basis set on the form of the exchange-correlation functional of the effective Kohn−Sham potential, and a comparison of the resulting shifts with the reference EOMCC,A data.

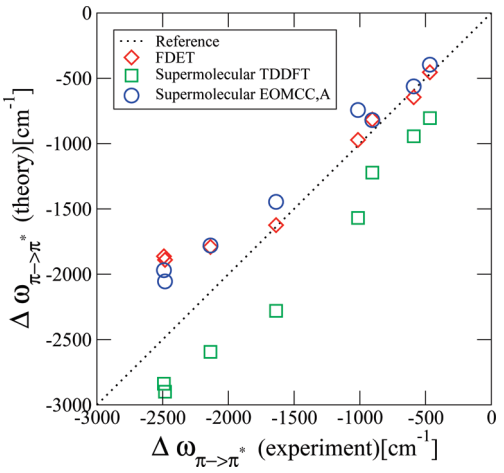

Figure 5. A comparison of the environment-induced shifts $\Delta\omega_{\pi\rightarrow\pi^*}$ of the vertical excitation energy corresponding to the lowest $\pi \rightarrow \pi^*$ transition in the *cis*-7HQ chromophore and resulting from the FDET with nonrelaxed-ρ_B and supermolecular TDDFT calculations using the STO ATZ2P basis set, with the reference supermolecular EOMCC,A and experimental[5] data (the latter obtained with laser resonant two-photon ionization UV spectroscopy).

are too large for performing such calculations on our computers. Thus, in the absence of the δ-CR-EOMCC(2,3) larger basis set data and considering the fact that the triples corrections to the environment-induced shifts $\Delta\omega_{\pi\rightarrow\pi^*}$ are relatively small when compared to the EOMCCSD $\Delta\omega_{\pi\rightarrow\pi^*}$ values, we have decided to combine the EOMCCSD/6-311+G(d) results with the triples corrections to EOMCCSD energies extracted from the δ-CR-EOMCC(2,3)/6-31+G(d) calculations, as in eq 32. As shown in Table 2, the resulting composite EOMCC,A and EOMCC,D approaches provide vertical excitation energies $\omega_{\pi\rightarrow\pi^*}$ that are in excellent agreement with the experimental excitation energies, while offering further improvements in the environment-induced shifts $\Delta\omega_{\pi\rightarrow\pi^*}$ when compared with the EOMCCSD/6-311+G(d) and δ-CR-EOMCC(2,3)/6-31+G(d) calculations. Indeed, the EOMCC,A approach, which adds the triples correction extracted from the δ-CR-EOMCC(2,3),A/6-31+G(d) calculation to the EOMCCSD/6-311+G(d) energy, gives errors in the calculated excitation energies $\omega_{\pi\rightarrow\pi^*}$ relative to experimental results that range between 147 cm^{-1} in the case of the bare *cis*-7HQ system and 668 cm^{-1} in the case of the 7HQ···(NH_3−H_2O−H_2O) complex, never exceeding 2% of the experimental excitation energies. The EOMCC,D approach, which adds the triples correction obtained in the δ-CR-EOMCC(2,3),D/6-31+G(d) calculation to the EOMCCSD/6-311+G(d) energy, gives errors in the calculated excitation energies $\omega_{\pi\rightarrow\pi^*}$ relative to experimental results that range between 17 cm^{-1} in the case of the 7HQ···$(H_2O)_2$ complex and 361 cm^{-1} for 7HQ···(NH_3−H_2O−H_2O), or no more than 1% of the experimental values. These results should be compared to the much larger differences between the EOMCCSD/6-311+G(d) and experimental excitation energies that range between 14 and 17%. The complexation-induced spectral shifts $\Delta\omega_{\pi\rightarrow\pi^*}$ resulting from the EOMCC,A and EOMCC,D calculations agree with their experimental counterparts to within 5−27% or 15% on average in the case of EOMCC,A and 10−37% or 22% on average in the EOMCC,D case. The EOMCC,D approach, while bringing the excitation energies $\omega_{\pi\rightarrow\pi^*}$ to a much closer agreement with experimental results than the EOMCCSD/6-311+G(d) calculations, does not offer improvements in the calculated shifts $\Delta\omega_{\pi\rightarrow\pi^*}$. The composite EOMCC,A approach provides additional small improvements in the calculated $\Delta\omega_{\pi\rightarrow\pi^*}$ values, reducing the 7−33% errors relative to experiment obtained in the EOMCCSD/6-311+G(d) calculations to 5−27%. For this reason, we consider the EOMCC,A values of the spectral shifts $\Delta\omega_{\pi\rightarrow\pi^*}$ as the theoretical reference values for assessing the quality of the FDET and supermolecular TDDFT calculations, although the use of EOMCC,D would not change any of our main conclusions.

Clearly, a comparison of the purely electronic EOMCC and experimental data discussed above has limitations, since we would have to examine the effect of nuclear motion on the calculated EOMCCSD and δ-CR-EOMCC(2,3) excitation energies and use basis sets larger than 6-31+G(d) in the δ-CR-EOMCC(2,3) calculations to make more definitive statements, which we cannot do at this time within the EOMCC framework due to the size of systems examined in this work. To overcome this difficulty, we could try to combine the EOMCC and TDDFT or FDET data, using TDDFT or FDET to examine the role of nuclear geometries and vibrational motions and δ-CR-EOMCC(2,3) to provide electronic excitation energies. The problem is that this would defeat the main purpose of the present study, in which we want to objectively compare the purely electronic FDET and supermolecular TDDFT results for the complexation-induced spectral shifts $\Delta\omega_{\pi\rightarrow\pi^*}$ with the corresponding, also purely electronic, EOMCC data, using the best EOMCC approach we can afford and using the same nuclear geometries in all calculations. Thus, although there are limitations in our EOMCC calculations when compared with experimental results which the present study cannot completely overcome, we believe that the EOMCC,A results obtained by combining the EOMCCSD/6-311+G(d) excitation energies with the triples corrections extracted from the δ-CR-EOMCC(2,3),A/6-31+G(d) calculations, as in eq 32, are of sufficiently high quality to allow us to assess the quality of the FDET and supermolecular TDDFT methods in applications involving the environment-induced spectral shifts in complexes of *cis*-7HQ.

4.2. A Comparison of the Excitation Energy Shifts from the FDET Calculations Using Nonrelaxed Environment Densities with the Reference EOMCC Data. As shown in Table 2 and in agreement with the experimental data,[5] the excitation energy shifts $\Delta\omega_{\pi\rightarrow\pi^*}$ for the hydrogen-bonded 7HQ$\cdots B$ complexes examined in this work resulting from the EOMCC calculations are always negative. Although this is not a strict rule, the magnitude of $\Delta\omega_{\pi\rightarrow\pi^*}$ correlates, to a large extent, with the size of the hydrogen-bonded environment B in the *cis*-7HQ$\cdots B$ complex. According to the reference EOMCC,A calculations, the shifts in the vertical excitation energy $\omega_{\pi\rightarrow\pi^*}$ corresponding to the lowest $\pi \rightarrow \pi^*$ transition in the *cis*-7HQ chromophore vary from -396 to -820 cm^{-1} in the case of the smaller 7HQ$\cdots B$ complexes involving the CH_3OH, H_2O, HCOOH, and NH_3 monomers, through -1446 cm^{-1} in the case of the 7HQ$\cdots(H_2O)_2$ complex involving the water dimer, to -1780 to -2055 cm^{-1} in the case of the largest 7HQ$\cdots B$ systems involving the $(NH_3-H_2O-NH_3)$, $(NH_3-H_2O-H_2O)$, and $(NH_3-NH_3-H_2O)$ trimers. It is interesting to examine how well the FDET and supermolecular TDDFT calculations reproduce these data.

We begin our discussion by assessing the quality of the FDET results employing the nonrelaxed density ρ_B, which is obtained by solving the Kohn−Sham equations for the environment molecule(s) in the absence of the *cis*-7HQ chromophore, with a focus on the results obtained with the monomer basis expansions to represent the chromophore density ρ_A and the environment density ρ_B. As explained in section 3.2, the combined use of the nonrelaxed environment density ρ_B and monomer expansions in the FDET calculations relies on the simplifying assumptions that the response of system AB to the process of electronic excitation is limited to chromophore A, that the coupling between the excitations in the embedded system and its environment can be neglected, and that the polarization of the environment molecules by the chromophore is of no importance. The supermolecular EOMCC calculations performed in this work do not rely on any of these assumptions, so a comparison of the FDET results employing the nonrelaxed density ρ_B and monomer expansions of ρ_A and ρ_B with the EOMCC data is particularly interesting.

As shown in Table 3 and Figure 2, the overall agreement of the monomer-expansion-based FDET/ATZ2P data using the nonrelaxed ρ_B with the reference EOMCC,A data is excellent. The absolute values of the deviations between the $\Delta\omega_{\pi\rightarrow\pi^*}$ values resulting from the nonrelaxed, monomer-expansion-based FDET/ATZ2P and supermolecular EOMCC,A calculations range from 4 cm^{-1} in the case of the 7HQ$\cdots NH_3$ complex, where the EOMCC,A shift is -820 cm^{-1}, to 229 cm^{-1} in the case of the 7HQ$\cdots$HCOOH system, where the EOMCC,A result for $\Delta\omega_{\pi\rightarrow\pi^*}$ is -743 cm^{-1}. The mean signed and unsigned errors in the nonrelaxed, monomer-expansion-based FDET/ATZ2P results for the environment-induced shifts $\Delta\omega_{\pi\rightarrow\pi^*}$ relative to the EOMCC,A reference data are -36 and 104 cm^{-1}, respectively, or 11%, if we average the individual relative errors. On the basis of the analysis of the EOMCCSD and δ-CR-EOMCC(2,3) calculations presented in section 4.1, the deviations between the nonrelaxed, monomer-expansion-based FDET/ATZ2P and reference EOMCC,A data shown in Table 3 and Figure 2 are well within the accuracy of the EOMCC calculations, indicating the excellent performance of the nonrelaxed FDET approach.

Remarkably, the nonrelaxed, monomer-expansion-based FDET values of the $\Delta\omega_{\pi\rightarrow\pi^*}$ shifts do not vary with the basis set (see Table 3−6), allowing us to obtain reasonably well converged results with the relatively small basis sets, such as STO DZP (cf. Table 6). Moreover, although we prefer to use the monomer expansion within the FDET approach, where the orbitals of the chromophore A and the corresponding density ρ_A are represented using the atomic centers of A, whereas the environment density ρ_B is represented using the atomic centers of B, the use of the supermolecular expansion within the FDET methodology employing the nonrelaxed ρ_B does not seem to change the calculated shift values. For example, as a comparison of the results shown in Tables 3 and 6 demonstrates, the average deviation from EOMCC,A characterizing the nonrelaxed, monomer-expansion-based FDET calculations using the smallest STO DZP basis set, of 115 cm^{-1}, is virtually identical to the analogous average deviation characterizing the nonrelaxed, supermolecular-expansion-based FDET calculations using the largest STO ATZ2P basis (108 cm^{-1}). It is also worth mentioning that the quality of the shifts calculated with the FDET approach using the nonrelaxed environment density ρ_B does not diminish with or significantly depend on the size of the environment. For example, the absolute value of the difference between the $\Delta\omega_{\pi\rightarrow\pi^*}$ values resulting from the nonrelaxed, monomer-expansion-based FDET/ATZ2P and supermolecular EOMCC,A calculations for the smallest 7HQ$\cdots H_2O$ complex is 83 cm^{-1} or 15%. The analogous difference characterizing the considerably larger 7HQ$\cdots(NH_3-H_2O-NH_3)$ complex is 11 cm^{-1} or 1%.

All of the above observations show that the FDET approach employing the nonrelaxed environment densities ρ_B, including its simplest, monomer-expansion-based variant, is as accurate in describing complexation-induced shifts as the high-level EOMCC approach with singles, doubles, and noniterative triples, represented here by the composite EOMCC,A approximation. The FDET results with relaxed densities ρ_B are discussed next.

4.3. The Dependence of the FDET Shifts on the Choice of ρ_B. By determining the environment density ρ_B in the absence of the chromophore, the nonrelaxed FDET model examined in section 4.2 ignores the complexation-induced changes in the electronic density of the environment, such as polarization of the environment molecule(s) by the chromophore. Furthermore, the use of monomer basis expansions to represent the chromophore density ρ_A and the environment density ρ_B does not allow for a penetration of the region of space occupied by the chromophore by the electronic density of the environment or for a penetration of space occupied by the environment by the electronic density of the chromophore. These simplifying assumptions make the nonrelaxed, monomer-expansion-based FDET approach computationally very attractive, as the costs of such calculations are defined by the size of the chromophore only. However, they represent an arbitrary choice, prompting the question of whether relaxing the environment density ρ_B in the presence of the chromophore would help the FDET results.

As explained in section 3.2, for a given choice of approximants for the functionals used in the FDET calculations, one can optimize the environment density ρ_B, adjusting it to the density of the chromophore ρ_A, when solving the Kohn−Sham-like system for the chromophore A embedded in the environment B defined by eq 13, by exploiting the "freeze-and-thaw" procedure.[80] One might think that such relaxed FDET calculations should be more accurate than the nonrelaxed ones in which ρ_B is not adjusted, since relaxation of ρ_B takes into account the effect of electronic polarization of the environment by the chromophore. Unfortunately, this is not necessarily the case

because of the inaccuracies in describing the nonadditive kinetic energy potential $v_t^{nad}[\rho_A,\rho_B](\vec{r})$, eq 12, that couples the two densities and that enters eq 13, especially when the full, supermolecular set of atomic orbitals, including those centered on *A* and those centered on *B*, is used to represent the chromophore density ρ_A and the environment density ρ_B.[64,84,130,131] It is usually impossible to *a priori* determine which effect is numerically more important in a molecular system of interest, the neglect of the electronic polarization of the environment by the chromophore or the errors produced by the approximations used to define the $v_t^{nad}[\rho_A,\rho_B](\vec{r})$ potential. In order to examine this issue, we performed the FDET calculations in which the environment density ρ_B was relaxed in the iterative process of solving eq 13 for the orbitals of the *cis*-7HQ chromophore.

As shown in Tables 3−6 and Figure 3, the relaxation of the environment density ρ_B in the FDET calculations for each of the eight complexes examined in this study substantially worsens the results for the $\Delta\omega_{\pi\rightarrow\pi^*}$ shifts when compared with the EOMCC,A reference data. The differences between the $\Delta\omega_{\pi\rightarrow\pi^*}$ values resulting from the relaxed FDET calculations using the STO ATZ2P basis set and the corresponding EOMCC,A data range, in absolute value, from 185 cm^{-1} in the case of the 7HQ···NH_3 complex, where the EOMCC,A shift is −820 cm^{-1}, to 569 cm^{-1}, in the case of the 7HQ···HCOOH system, where the EOMCC,A result for $\Delta\omega_{\pi\rightarrow\pi^*}$ is −743 cm^{-1}. These are much larger differences when compared with the corresponding nonrelaxed FDET calculations, which, as pointed out in section 4.2, give substantially smaller differences with the EOMCC,A data that range from 4 to 229 cm^{-1} when the same basis set is employed. As shown in Table 3, the mean signed and unsigned errors in the relaxed FDET/ATZ2P results for the environment-induced shifts $\Delta\omega_{\pi\rightarrow\pi^*}$ relative to the EOMCC,A reference data are −366 and 366 cm^{-1}, respectively, or, if we average the individual relative errors, 37%. This should be contrasted with the mean signed error of −36 cm^{-1}, mean unsigned error of 104 cm^{-1}, and average relative error of 11% in the analogous nonrelaxed FDET calculations. In some cases, the effect of relaxing ρ_B in the FDET calculations on the calculated $\Delta\omega_{\pi\rightarrow\pi^*}$ shifts is enormous, e.g., 546 cm^{-1} in the 7HQ···(NH_3−NH_3−H_2O) case. As in the case of the FDET calculations using the nonrelaxed densities ρ_B, neither the type of the basis expansion used to represent densities ρ_A and ρ_B (monomer or supermolecular) nor the computational basis set used in the calculations affect the above observations (see Tables 3−6), although the use of the supermolecular expansion to represent ρ_A and ρ_B in the context of the relaxed FDET calculations with the STO ATZ2P basis set seems to worsen the results, increasing the mean unsigned error in the calculated $\Delta\omega_{\pi\rightarrow\pi^*}$ values relative to EOMCC,A from 366 cm^{-1} in the monomer-expansion case to 486 cm^{-1}, when the supermolecular expansion is employed (cf. the results in Tables 3 and 4), bringing the relaxed FDET results closer to the supermolecular TDDFT data (cf. the discussion below).

The substantial increase in the differences between the FDET and EOMCC,A shift values due to the relaxation of the environment densities ρ_B may be related to the fact that the Kohn−Sham-type methods applying semilocal approximants to the exchange-correlation energy used in this work tend to overestimate molecular polarizabilities in organic molecules.[132,133] The exaggerated polarizability values would certainly lead to the overestimated chromophore polarization effects that could result in the artificially enhanced effects of relaxation of environment densities on the calculated $\Delta\omega_{\pi\rightarrow\pi^*}$ values observed in our calculations. We must remember though that this argument, although reasonable here, may not be generally applicable, since going to the left-hand side of the periodic table shows that the same functionals underestimate polarizabilities.[134]

It is worth pointing out that the result of the "freeze-and-thaw" FDET calculations employing the complete supermolecular basis expansion to represent the ρ_A and ρ_B densities, in which the environment density ρ_B is allowed to relax when solving eq 13 for the orbitals of *A*, represents the variational limit for a given approximant to the nonadditive kinetic energy potential $v_t^{nad}[\rho_A,\rho_B](\vec{r})$. If such an approximant were exact and if the same approximant were used to represent all of the exchange-correlation contributions in both supermolecular TDDFT and FDET calculations, the total electron density obtained in the relaxed "freeze-and-thaw" FDET calculations and its analog obtained in the supermolecular TDDFT calculations would be identical (see ref 48 and the references therein). This explains why the results of the relaxed FDET calculations using the supermolecular basis expansions to represent the ρ_A and ρ_B densities and their supermolecular TDDFT analogs shown in Table 4 and Figure 3 are so similar. Indeed, by relaxing the ρ_A and ρ_B densities simultaneously and by allowing them to penetrate both subsystems *A* and *B* when solving eq 13, we produce the situation in which the differences between the supermolecular and embedding strategies for calculating the $\Delta\omega_{\pi\rightarrow\pi^*}$ shifts become small. We must remember though that by relaxing the environment densities in the FDET approach or by performing the supermolecular TDDFT calculations with the functionals that are certainly imperfect, we introduce new errors, such as the inadequacy of the representation of the nonadditive kinetic energy potential $v_t^{nad}[\rho_A,\rho_B](\vec{r})$ in the FDET considerations that may be significantly enhanced when ρ_B is relaxed or the difficulties with maintaining a balanced treatment of the chromophore and its complex with the environment within the supermolecular TDDFT framework. These are the reasons why the nonrelaxed FDET approach may represent a better computational strategy in determining the excitation energy shifts in weakly bound systems of the type of complexes examined in this work, when compared with the relaxed FDET and supermolecular TDDFT methodologies, as the results in Tables 3−6 and Figures 2−5 clearly illustrate.

4.4. A Comparison of the Excitation Energy Shifts from the Supermolecular TDDFT Calculations with the Nonrelaxed FDET and Reference EOMCC Data. As already alluded to above, the excitation energy shifts in the eight complexes of *cis*-7HQ examined in this study resulting from the supermolecular TDDFT calculations are a lot less accurate than their FDET counterparts employing the nonrelaxed environment densities, when both types of calculations are compared with the reference EOMCC,A data. They are also less accurate than the FDET results obtained with the relaxed environment densities, although, as pointed out at the end of section 4.3, the differences between the $\Delta\omega_{\pi\rightarrow\pi^*}$ values obtained in the supermolecular TDDFT and relaxed FDET calculations are smaller than the analogous differences between the results of the supermolecular TDDFT and nonrelaxed FDET calculations. Indeed, as shown in Table 3 (cf., also, Figure 3), the differences between the $\Delta\omega_{\pi\rightarrow\pi^*}$ shift values obtained in the supermolecular TDDFT calculations using the STO ATZ2P basis set and their reference EOMCC,A counterparts range, in absolute value, from 382 cm^{-1} in the case of the 7HQ···H_2O complex, where the EOMCC,A shift

is -562 cm^{-1}, to 869 cm^{-1}, in the case of the 7HQ$\cdots$($NH_3-H_2O-H_2O$) system, where the EOMCC,A $\Delta\omega_{\pi\rightarrow\pi^*}$ value is -1969 cm^{-1}. The mean unsigned error in the supermolecular TDDFT/ATZ2P values of the $\Delta\omega_{\pi\rightarrow\pi^*}$ shifts relative to EOMCC,A is 673 cm^{-1} or, if we average the individual relative errors, 65%. These clearly are much larger differences when compared with the corresponding nonrelaxed, monomer-expansion-based FDET calculations that give the 4$-$229 cm^{-1} deviations from the EOMCC,A data and the differences, which are about twice as large as those characterizing the relaxed, monomer-expansion-based FDET approach. The 65% average relative error characterizing the $\Delta\omega_{\pi\rightarrow\pi^*}$ values resulting from the supermolecular TDDFT/ATZ2P calculations is 6 times bigger than the analogous error characterizing the nonrelaxed, monomer-expansion-based FDET/ATZ2P calculations. On the basis of the analysis of the EOMCC calculations performed in this work presented in section 4.1, the differences between the supermolecular TDDFT and reference EOMCC,A data are well outside the accuracy of the EOMCC calculations for the $\Delta\omega_{\pi\rightarrow\pi^*}$ shifts, indicating the poor performance of the supermolecular TDDFT approach. Unlike in the FDET case, the differences between the supermolecular TDDFT and EOMCC,A $\Delta\omega_{\pi\rightarrow\pi^*}$ values increase with the size of the environment bound to the *cis*-7HQ chromophore. This indicates the difficulties with obtaining the balanced description of excitation energies in systems that have different sizes in the supermolecular TDDFT calculations, which are not present in the FDET and EOMCC calculations.

The large inaccuracies in the supermolecular TDDFT results might be due to various reasons. One possibility might be the basis set superposition error (BSSE), which could potentially be well pronounced due to the difficulties the supermolecular TDDFT approach has with obtaining a balanced description of excitation energies in systems that have different sizes, but, as shown in Table 7, the $\pi\rightarrow\pi^*$ excitation energy in the isolated *cis*-7HQ system is barely affected by the position of ghost basis functions centered on the atoms of environment molecules. Another possibility might be a particular choice of the approximation used to determine the exchange-correlation potential contributions in the TDDFT calculations (the SAOP scheme[129]). To investigate this issue, we performed additional supermolecular TDDFT calculations using two other treatments of the exchange-correlation contributions, namely, the local density approximation (LDA)[135] and the PW91 functional,[136] which is a representative functional from the GGA family. The results of these additional calculations are shown in Table 8 and Figure 4. It is quite clear that the use of the LDA and PW91 functionals to treat the exchange-correlation contributions does not help the supermolecular TDDFT results, making them, in fact, even less accurate than in the SAOP case. Interestingly, the use of the LDA and PW91 functionals in the nonrelaxed FDET calculations has a small effect on these calculations, increasing the mean unsigned errors relative to EOMCC,A characterizing the SAOP-based nonrelaxed, monomer-expansion-based FDET/ATZ2P calculations of 104 cm^{-1} to 140 cm^{-1} in the LDA case and 149 cm^{-1} in the PW91 case. This makes us believe that the primary reason for the poor performance of the supermolecular TDDFT approach is the difficulty with obtaining a balanced description of excitation energies in systems that have different sizes in the supermolecular TDDFT calculations, which are not present in the size-intensive FDET and EOMCC calculations and which are only enhanced in the supermolecular TDDFT calculations by incorrect asymptotic behavior of the LDA and PW91 (GGA) potentials, critical for the determination of the relatively small spectral shifts in weakly bound molecular clusters. This is yet another argument in favor of the embedding strategy represented here by the FDET approach, which is much less sensitive to the asymptotic behavior of the exchange-correlation potentials.

4.5. A Comparison of the Excitation Energy Shifts from the FDET Calculations Using Nonrelaxed Environment Densities with the Experimental Data. Although the main goal of this work is to compare the FDET and supermolecular TDDFT values of the vertical excitation energy shifts characterizing the hydrogen-bonded complexes of the *cis*-7HQ system with the corresponding EOMCC,A data, all obtained using the same nuclear geometries, it is useful to comment on the quality of the shifts resulting from our best FDET calculations employing the nonrelaxed environment densities, when compared with the available experimental data.[5] In analogy to the EOMCC,A results discussed in section 4.1, a comparison of the purely electronic FDET and experimental data discussed above has limitations, since one cannot measure vertical excitation energies obtained in the FDET calculations in a direct manner. The experimental shifts reported in ref 5 that we refer to in this work correspond to the complexation-induced shifts in the maxima of the $\pi\rightarrow\pi^*$ absorption band in the cis-7HQ chromophore. Thus, although the experimental shifts reported in ref 5 are closely related to the theoretical shifts obtained in this study, the two types of quantities differ because of the following factors: (i) the maxima of the absorption bands characterizing the isolated *cis*-7HQ system and its complexes may not occur between the same vibrational levels as a result of the geometry relaxation in the excited states of the *cis*-7HQ$\cdots B$ complexes when compared to the corresponding ground electronic states, and (ii) the MP2/aug-cc-pVTZ geometries of *cis*-7HQ and its complexes used in this work, although probably quite reasonable, are not the experimental geometries. All of these factors certainly contribute to the deviations between the theoretical shifts calculated in this study and their experimental counterparts reported in ref 5.

On the other hand, the careful EOMCC calculations reported in this work which, as analyzed in section 4.1, closely follow the experimental excitation energies corresponding to the lowest $\pi\rightarrow\pi^*$ transition in the *cis*-7HQ and *cis*-7HQ$\cdots B$ systems, particularly when the EOMCC,A and EOMCC,B approaches corrected for triple excitations are employed (see Table 2), seem to indicate that all of the above factors, although important, lead to a relatively small overall effect. It is, therefore, interesting to compare our best FDET results for the excitation energy shifts $\Delta\omega_{\pi\rightarrow\pi^*}$, obtained in the nonrelaxed, monomer-expansion-based FDET calculations employing the STO ATZ2P basis set, given in Table 3, which are in excellent agreement with the reference EOMCC,A data, with the experimentally derived shifts reported in ref 5 and listed in Table 2. This comparison is shown in Figure 5. As one can see by inspecting Tables 2 and 3 and Figure 5, the $\Delta\omega_{\pi\rightarrow\pi^*}$ values obtained in the nonrelaxed, monomer-expansion-based FDET/ATZ2P calculations are in very good agreement with the shifts in the experimental UV absorption spectra. The mean unsigned error in the $\Delta\omega_{\pi\rightarrow\pi^*}$ values resulting from the nonrelaxed, monomer-expansion-based FDET/ATZ2P calculations, relative to the spectral shifts observed in experiment, is 222 cm^{-1}, in excellent agreement with the EOMCC,A approach, which gives 244 cm^{-1}. The analogous mean unsigned error characterizing the supermolecular TDDFT calculations is twice as large (429 cm^{-1}), demonstrating once

again the advantages of the embedding vs supermolecular strategy within the TDDFT framework. It is clearly very encouraging that the nonrelaxed FDET approach, which can be applied to large molecular systems, can provide shifts in the excitation energy corresponding to the lowest $\pi \rightarrow \pi^*$ transition in the *cis*-7HQ system due to the formation of hydrogen-bonded complexes involving *cis*-7HQ and a variety of small molecules that can compete with the results of the considerably more expensive EOMCC calculations.

5. SUMMARY AND CONCLUSIONS

We used the embedding FDET approach to determine the shifts in the excitation energy corresponding to the lowest $\pi \rightarrow \pi^*$ transition in *cis*-7-hydroxyquinoline (*cis*-7HQ), induced by the formation of hydrogen-bonded complexes of *cis*-7HQ with a number of small molecules, and compared the resulting shift values with the reference EOMCC data and the analogous shifts obtained in the conventional supermolecular TDDFT calculations. The main difference between the embedding strategy, represented in the present study by the FDET method, and the conventional supermolecular approach is in the fact that in the former case one evaluates the excitation energy shifts induced by the interactions of the chromophore with its molecular environment as the differences of the excitation energies of the same many-electron system, representing the chromophore fragment with two different effective potentials, whereas in the latter case one has to perform calculations for two systems that differ in the number of electrons, the complex formed by the chromophore and its molecular environment, and the isolated chromophore.

By considering eight complexes of *cis*-7HQ with up to three small hydrogen-bonded molecules, we demonstrated that the spectral shifts resulting from the FDET calculations with the *a priori* determined nonrelaxed environment densities are in excellent agreement with the reference EOMCC data obtained in the supermolecular, rigorously size-intensive EOMCC calculations with singles, doubles, and noniterative triples, whereas the analogous shifts obtained with the supermolecular TDDFT approach are far from those obtained with EOMCC. The nonrelaxed FDET calculations provide shifts that agree with their EOMCC analogs to within about 100 cm^{-1} or 10% on average, where the absolute values of the excitation energy shifts in the complexes of *cis*-7HQ examined in this study resulting from the EOMCC calculations range between about 500 and 2000 cm^{-1}. As shown in the present study, the accuracy of the FDET shift calculations employing nonrelaxed environment densities is on the order of the accuracy of the high-level EOMCC calculations. This should be contrasted with the excitation energy shifts obtained with the supermolecular TDDFT approach, which differ from the reference EOMCC values reported in this work by about 700 cm^{-1} or 65% on average and which are well outside the accuracy of the EOMCC calculations. We demonstrated that none of the above findings are significantly affected by the type of basis expansion used in the FDET calculations (monomer or supermolecular), by the computational basis set used in the FDET and supermolecular TDDFT calculations, or by the approximations applied to the exchange-correlation potentials in the FDET and supermolecular TDDFT calculations, although it is quite clear that better approximations for the exchange-correlation potential would help the supermolecular TDDFT approach. One of the key findings of the present study is the fact that the FDET methodology, particularly the nonrelaxed form of it, works well even with the functionals that are characterized by the relatively poor long-range behavior, offering results that are competitive with the high-level EOMCC approaches.

We demonstrated that the relaxation of the environment density in the FDET calculations worsens the quality of the calculated spectral shifts, although the shifts resulting from the relaxed FDET calculations are typically somewhat more accurate than those obtained with the supermolecular TDDFT approach. Among the reasons that may contribute to the worsening of the results obtained with the FDET approach using relaxed environment densities are the difficulties the Kohn−Sham-type methods applying semilocal approximants to the exchange-correlation energy, used in this work, have with describing molecular polarizabilities and the inadequacies in representing the nonadditive kinetic energy potential in the FDET considerations that may be significantly enhanced when the environment density is allowed to relax when solving a coupled system of Kohn−Sham-like equations defining the FDET approach and involving the chromophore and environment densities. Our calculations strongly suggest that at least in the applications involving shifts in the electronic spectrum due to the formation of weakly bound complexes, where the electronic excitation is localized on the absorbing chromophore, the neglect of the electronic polarization of the environment by the chromophore, implicitly assumed in the FDET calculations using nonrelaxed environment densities, is of much lesser significance than the errors that result from the approximations used to define the nonadditive kinetic energy potential, which can be quite substantial. On the basis of a direct comparison of the FDET results obtained with nonrelaxed and relaxed environment densities, the nonrelaxed FDET approach is a preferred strategy for the embedding calculations if the polarization of the environment by the chromophore is small, as is the case when the weakly bound complexes of *cis*-7HQ are examined. On the other hand, if one is interested in generating results that are similar to those obtained with the supermolecular TDDFT methodology, relaxing environment density in the FDET calculations may be more appropriate. We demonstrated that the fully relaxed FDET calculations are capable of producing spectral shifts that are quite close to the results of the supermolecular TDDFT calculations, even though both sets of calculations led to results that are quite far from the benchmark EOMCC and experimental data.

As shown in our study, the FDET approach with nonrelaxed environment densities represents a robust computational methodology, which works much better than the FDET methods with relaxed densities and supermolecular TDDFT schemes and which can provide complexation-induced spectral shifts that can compete with the high-quality *ab initio* data resulting from EOMCC calculations, as long as one can neglect the polarization of the environment by the chromophore. This is very encouraging from the point of view of spectroscopic applications involving large weakly bound molecular complexes, since the FDET approach with nonrelaxed environment densities is less expensive than its relaxed and supermolecular TDDFT counterparts, not to mention the EOMCC methods. In the FDET calculations employing nonrelaxed environment densities, one obtains these densities only once and *a priori* by solving the ground-state Kohn−Sham equations for the environment molecule(s) in the absence of the absorbing chromophore. This should be contrasted with the relaxed FDET calculations, where

the environment density is allowed to vary during the Kohn–Sham-like calculations for the orbitals of the chromophore embedded in the environment, and with the supermolecular TDDFT and EOMCC calculations, where one has to consider larger many-electron systems corresponding to the chromophore complexes that do not have to be considered in the FDET calculations. The latter is challenging for the supermolecular TDDFT approaches, since they have difficulties with balancing accuracies involving systems of different sizes, and for methods based on the EOMCC theory, which can balance these accuracies, but are often prohibitively expensive.

Although the main focus of this study was the comparison of the FDET and supermolecular TDDFT results for the complexation-induced shifts in the excitation energy corresponding to the lowest $\pi \rightarrow \pi^*$ transition in *cis*-7HQ with the EOMCC data, we also compared the FDET, supermolecular TDDFT, and reference EOMCC shift values with the experimental shifts reported in ref 5. Although, as explained in the previous sections, such comparison has obvious limitations due to the neglect of the effect of nuclear motion on photoabsorption spectra in our purely electronic calculations, the spectral shifts obtained with the FDET approach using nonrelaxed environment densities and those obtained with the EOMCC methodology agree with the experimental shifts quite well, whereas the supermolecular TDDFT calculations produce once again very large errors. This confirms the superiority of the FDET strategy when compared with the conventional supermolecular TDDFT approach in applications involving complexation-induced spectral shifts.

■ ASSOCIATED CONTENT

Supporting Information. The nuclear geometries of the cis-7HQ molecule and its complexes examined in this study along with the vertical excitation energies $\omega_{\pi\rightarrow\pi^*}$ resulting from the FDET and supermolecular TDDFT calculations. This material is available free of charge via the Internet at http://pubs.acs.org/.

■ AUTHOR INFORMATION

Corresponding Authors

*E-mail: tomasz.wesolowski@unige.ch; piecuch@chemistry.msu.edu.

■ ACKNOWLEDGMENT

This work has been supported by the Chemical Sciences, Geosciences and Biosciences Division, Office of Basic Energy Sciences, Office of Science, U.S. Department of Energy (Grant No. DE-FG02-01ER15228; P.P.) and Fonds National Suisse de la Recherche Scientifique (Grant No. 200020-124817; T.A.W.).

■ REFERENCES

(1) Tanner, C.; Manca, C.; Leutwyler, S. *Science* **2003**, *302*, 1736.
(2) Bruhwiler, D.; Calzaferri, G.; Torres, T.; Ramm, J. H.; Gartmann, N.; Dieu, L.-Q.; Lopez-Duarte, I.; Martinez-Diaz, M. V. *J. Mater. Chem.* **2009**, *19*, 8040.
(3) Hernandez, F. E.; Yu, S.; Garcia, M.; Campiglia, A. D. *J. Phys. Chem. B* **2005**, *109*, 9499.
(4) Goldberg, J. M.; Batjargal, S.; Petersson, E. J. *J. Am. Chem. Soc.* **2010**, *132*, 14719.
(5) Thut, M.; Tanner, C.; Steinlin, A.; Leutwyler, S. *J. Phys. Chem. A* **2008**, *112*, 5566.
(6) Emrich, K. *Nucl. Phys. A* **1981**, *351*, 379.
(7) Geertsen, J.; Rittby, M.; Bartlett, R. J. *Chem. Phys. Lett.* **1989**, *164*, 57.
(8) Comeau, D. C.; Bartlett, R. J. *Chem. Phys. Lett.* **1993**, *207*, 414.
(9) Stanton, J. F.; Bartlett, R. J. *J. Chem. Phys.* **1993**, *98*, 7029.
(10) Piecuch, P.; Bartlett, R. J. *Adv. Quantum Chem.* **1999**, *34*, 295.
(11) Monkhorst, H. *Int. J. Quantum Chem. Symp.* **1977**, *11*, 421.
(12) Dalgaard, E.; Monkhorst, H. *Phys. Rev. A* **1983**, *28*, 1217.
(13) Mukherjee, D.; Mukherjee, P. K. *Chem. Phys.* **1979**, *39*, 325.
(14) Takahashi, M.; Paldus, J. *J. Chem. Phys.* **1986**, *85*, 1486.
(15) Koch, H.; Jørgensen, P. *J. Chem. Phys.* **1990**, *93*, 3333.
(16) Koch, H.; Jensen, H. J. A.; Jørgensen, P.; Helgaker, T. *J. Chem. Phys.* **1990**, *93*, 3345.
(17) Coester, F. *Nucl. Phys.* **1958**, *7*, 421.
(18) Coester, F.; Kümmel, H. *Nucl. Phys.* **1960**, *17*, 477.
(19) Čížek, J. *J. Chem. Phys.* **1966**, *45*, 4256.
(20) Čížek, J. *Adv. Chem. Phys.* **1969**, *14*, 35.
(21) Čížek, J.; Paldus, J. *Int. J. Quantum Chem.* **1971**, *5*, 359.
(22) Paldus, J.; Shavitt, I.; Čížek, J. *Phys. Rev. A* **1972**, *5*, 50.
(23) Gauss, J. In *Encyclopedia of Computational Chemistry*; Schleyer, P.v.R., Allinger, N. L., Clark, T., Gasteiger, J., Kollman, P. A., Schaefer, H. F., III, Schreiner, P. R., Eds.; Wiley: Chichester, U. K., 1998; Vol. 1; pp 615–636.
(24) Paldus, J.; Li, X. *Adv. Chem. Phys.* **1999**, *110*, 1.
(25) Bartlett, R. J.; Musiał, M. *Rev. Mod. Phys.* **2007**, *79*, 291.
(26) Piecuch, P.; Włoch, M. *J. Chem. Phys.* **2005**, *123*, 224105.
(27) Piecuch, P.; Włoch, M.; Gour, J. R.; Kinal, A. *Chem. Phys. Lett.* **2006**, *418*, 467.
(28) Włoch, M.; Gour, J. R.; Piecuch, P. *J. Phys. Chem. A* **2007**, *111*, 11359.
(29) Włoch, M.; Lodriguito, M. D.; Piecuch, P.; Gour, J. R. *Mol. Phys.* **2006**, *104*, 2149.
(30) Piecuch, P.; Gour, J. R.; Włoch, M. *Int. J. Quantum Chem.* **2009**, *109*, 3268.
(31) Shiozaki, T.; Hirao, K.; Hirata, S. *J. Chem. Phys.* **2007**, *126*, 244106.
(32) Watts, J. D.; Bartlett, R. J. *Chem. Phys. Lett.* **1996**, *258*, 581.
(33) Meissner, L.; Bartlett, R. J. *J. Chem. Phys.* **1995**, *102*, 7490.
(34) Korona, T.; Werner, H.-J. *J. Chem. Phys.* **2003**, *118*, 3006.
(35) Korona, T.; Schütz, M. *J. Chem. Phys.* **2006**, *125*, 104106.
(36) Kats, D.; Korona, T.; Schütz, M. *J. Chem. Phys.* **2007**, *127*, 064107.
(37) Crawford, T. D.; King, R. A. *Chem. Phys. Lett.* **2002**, *366*, 611.
(38) Fan, P.-D.; Valiev, M.; Kowalski, K. *Chem. Phys. Lett.* **2008**, *458*, 205.
(39) Valiev, M.; Kowalski, K. *J. Chem. Phys.* **2006**, *125*, 211101.
(40) Valiev, M.; Kowalski, K. *J. Phys. Chem. A* **2006**, *110*, 13106.
(41) Kowalski, K.; Valiev, M. *J. Phys. Chem. A* **2008**, *112*, 5538.
(42) Epifanovsky, E.; Kowalski, K.; Fan, P.-D.; Valiev, M.; Matsika, S.; Krylov, A. I. *J. Phys. Chem. A* **2008**, *112*, 9983.
(43) Li, W.; Gour, J. R.; Piecuch, P.; Li, S. *J. Chem. Phys.* **2009**, *131*, 114109.
(44) Li, W.; Piecuch, P. *J. Phys. Chem. A* **2010**, *114*, 8644.
(45) Li, W.; Piecuch, P. *J. Phys. Chem. A* **2010**, *114*, 6721.
(46) Casida, M. E. In *Recent Advances in Density-Functional Methods, Part-I*; Chong, D. P., Ed.; World Scientific: Singapore, 1995; pp 155–192.
(47) Wesolowski, T. A.; Warshel, A. *J. Phys. Chem.* **1993**, *97*, 8050.
(48) Wesołowski, T. A. In *Computational Chemistry: Reviews of Current Trends*; Leszczyński, J., Ed.; World Scientific: Singapore, 2006; Vol. 10; pp 1–82.
(49) Wesolowski, T. A. *Phys. Rev. A* **2008**, *77*, 012504.
(50) Pernal, K.; Wesolowski, T. A. *Int. J. Quantum Chem.* **2009**, *109*, 2520.
(51) Wesolowski, T. A.; Warshel, A. *J. Phys. Chem.* **1994**, *98*, 5183.
(52) Neugebauer, J.; Louwerse, M. J.; Baerends, E. J.; Wesolowski, T. A. *J. Chem. Phys.* **2005**, *122*, 094115.
(53) Kaminski, J. W.; Gusarov, S.; Kovalenko, A.; Wesolowski, T. A. *J. Phys. Chem. A* **2010**, *114*, 6082.

(54) Savin, A.; Wesolowski, T. A. In *Advances in the Theory of Atomic and Molecular Systems: Conceptual and Computational Advances in Quantum Chemistry*; Piecuch, P., Maruani, J., Delgado-Barrio, G., Wilson, S., Eds.; Progress in Theoretical Chemistry and Physics; Springer: Dordrecht, The Netherlands, 2009; Vol. 19; pp 327−339.
(55) Roncero, O.; de Lara-Castells, M.; Villarreal, P.; Flores, F.; Ortega, J.; Paniagua, M.; Aguado, A. *J. Chem. Phys.* **2008**, *129*, 184104.
(56) Fux, S.; Jacob, C.; Neugebauer, J.; Visscher, L.; Reiher, M. *J. Chem. Phys.* **2010**, *132*, 164101.
(57) Goodpaster, J. D.; Ananth, N.; Manby, F. R.; Miller, T. F., III. *J. Chem. Phys.* **2010**, *133*, 084103.
(58) Wesolowski, T. *J. Am. Chem. Soc.* **2004**, *126*, 11444.
(59) Fradelos, G.; Kaminski, J. W.; Wesolowski, T. A.; Leutwyler, S. *J. Phys. Chem. A* **2009**, *19*, 9766.
(60) Zbiri, M.; Atanasov, M.; Daul, C.; Garcia-Lastra, J. M.; Wesolowski, T. A. *Chem. Phys. Lett.* **2004**, *397*, 441.
(61) Fradelos, G.; Wesolowski, T. A. *J. Chem. Theory Comput.* **2011**, *7*, 213.
(62) Domcke, W.; Sobolewski, A. L. *Science* **2003**, *302*, 1963.
(63) Wesolowski, T. A. *J. Am. Chem. Soc.* **2004**, *126*, 11444.
(64) Lastra, J. M. G.; Kaminski, J. W.; Wesolowski, T. A. *J. Chem. Phys.* **2008**, *129*, 074107.
(65) Stefanovich, E. V.; Truong, T. N. *J. Chem. Phys.* **1996**, *104*, 2946.
(66) Govind, N.; Wang, Y. A.; Carter, E. A. *J. Chem. Phys.* **1999**, *110*, 7677.
(67) Neugebauer, J.; Jacob, C. R.; Wesolowski, T. A.; Baerends, E. J. *J. Phys. Chem. A* **2005**, *109*, 7805.
(68) Hodak, M.; Lu, W.; Bernholc, J. *J. Chem. Phys.* **2008**, *128*, 014101.
(69) Gomes, A. S. P.; Jacob, C. R.; Visscher, L. *Phys. Chem. Chem. Phys.* **2008**, *10*, 5353.
(70) Kohn, W.; Sham, L. J. *Phys. Rev.* **1965**, *140*, A1133.
(71) Hohenberg, P.; Kohn, W. *Phys. Rev.* **1964**, *136*, B864.
(72) Wesolowski, T. A. *Chem. Phys. Lett.* **1999**, *311*, 87.
(73) Neugebauer, J.; Louwerse, M. J.; Belanzoni, P.; Wesolowski, T. A.; Baerends, E. J. *J. Chem. Phys.* **2005**, *123*, 114101.
(74) Jacob, C. R.; Visscher, L. *J. Chem. Phys.* **2006**, *125*, 194104.
(75) Jacob, C. J.; Neugebauer, J.; Jensen, L.; Visscher, L. *Phys. Chem. Chem. Phys.* **2006**, *8*, 2349.
(76) Cortona, P. *Phys. Rev. B* **1991**, *44*, 8454.
(77) Senatore, G.; Subbaswamy, K. *Phys. Rev. B* **1986**, *34*, 5754.
(78) Elliott, P.; Cohen, M. H.; Wasserman, A.; Burke, K. *J. Chem. Theory Comput.* **2009**, *5*, 827.
(79) Iannuzzi, M.; Kirchner, B.; Hutter, J. *Chem. Phys. Lett.* **2006**, *421*, 16.
(80) Wesolowski, T. A.; Weber, J. *Chem. Phys. Lett.* **1996**, *248*, 71.
(81) Wesolowski, T. A.; Tran, F. *J. Chem. Phys.* **2003**, *118*, 2072.
(82) Kevorkyants, R.; Dulak, M.; Wesolowski, T. A. *J. Chem. Phys.* **2006**, *124*, 024104.
(83) Dulak, M.; Kaminski, J. W.; Wesolowski, T. A. *J. Chem. Theory Comput.* **2007**, *3*, 735.
(84) Wesolowski, T. A.; Weber, J. *Int. J. Quantum Chem.* **1997**, *61*, 303.
(85) Bernard, Y. A.; Dulak, M.; Kaminski, J. W.; Wesolowski, T. A. *J. Phys. A* **2008**, *41*, 0553902.
(86) Dulak, M.; Kaminski, J. W.; Wesolowski, T. A. *Int. J. Quant. Chem.* **2009**, *109*, 1886.
(87) Piecuch, P.; Kowalski, K.; Pimienta, I. S. O.; McGuire, M. J. *Int. Rev. Phys. Chem.* **2002**, *21*, 527.
(88) Piecuch, P.; Kowalski, K.; Pimienta, I. S. O.; Fan, P.-D.; Lodriguito, M.; McGuire, M. J.; Kucharski, S. A.; Kuś, T.; Musiał, M. *Theor. Chem. Acc.* **2004**, *112*, 349.
(89) Kowalski, K.; Piecuch, P. *J. Chem. Phys.* **2001**, *115*, 2966.
(90) Kowalski, K.; Piecuch, P. *J. Chem. Phys.* **2002**, *116*, 7411.
(91) Kowalski, K.; Piecuch, P. *J. Chem. Phys.* **2004**, *120*, 1715.
(92) Włoch, M.; Gour, J. R.; Kowalski, K.; Piecuch, P. *J. Chem. Phys.* **2005**, *122*, 214107.
(93) Kowalski, K.; Hirata, S.; Włoch, M.; Piecuch, P.; Windus, T. L. *J. Chem. Phys.* **2005**, *123*, 074319.
(94) Coussan, S.; Ferro, Y.; Trivella, A.; Roubin, P.; Wieczorek, R.; Manca, C.; Piecuch, P.; Kowalski, K.; Włoch, M.; Kucharski, S. A.; Musiał, M. *J. Phys. Chem. A* **2006**, *110*, 3920.
(95) Kowalski, K.; Krishnamoorthy, S.; Villa, O.; Hammond, J. R.; Govind, N. *J. Chem. Phys.* **2010**, *132*, 154103.
(96) Kowalski, K.; Piecuch, P. *J. Chem. Phys.* **2001**, *115*, 643.
(97) Kowalski, K.; Piecuch, P. *Chem. Phys. Lett.* **2001**, *347*, 237.
(98) Kucharski, S. A.; Włoch, M.; Musiał, M.; Bartlett, R. J. *J. Chem. Phys.* **2001**, *115*, 8263.
(99) Kowalski, K.; Piecuch, P. *J. Chem. Phys.* **2000**, *113*, 8490.
(100) Hirata, S.; Nooijen, M.; Grabowski, I.; Bartlett, R. J. *J. Chem. Phys.* **2001**, *114*, 3919; **2001**, *115*, 3967 [Erratum].
(101) Watts, J. D.; Bartlett, R. J. *Chem. Phys. Lett.* **1995**, *233*, 81.
(102) Christiansen, O.; Koch, H.; Jørgensen, P. *J. Chem. Phys.* **1996**, *105*, 1451.
(103) Christiansen, O.; Koch, H.; Jørgensen, P.; Olsen, J. *Chem. Phys. Lett.* **1996**, *256*, 185.
(104) Koch, H.; Christiansen, O.; Jørgensen, P.; Olsen, J. *Chem. Phys. Lett.* **1995**, *244*, 75.
(105) Christiansen, O.; Koch, H.; Jørgensen, P. *J. Chem. Phys.* **1995**, *103*, 7429.
(106) Kowalski, K. *J. Chem. Phys.* **2009**, *130*, 194110.
(107) Manohar, P. U.; Krylov, A. I. *J. Chem. Phys.* **2008**, *129*, 194105.
(108) Raghavachari, K.; Trucks, G. W.; Pople, J. A.; Head-Gordon, M. *Chem. Phys. Lett.* **1989**, *102*, 479.
(109) Piecuch, P.; Kowalski, K. In *Computational Chemistry: Reviews of Current Trends*; Leszczyński, J., Ed.; World Scientific: Singapore, 2000; Vol. 5; pp 1−104.
(110) Kowalski, K.; Piecuch, P. *J. Chem. Phys.* **2000**, *113*, 18.
(111) Kowalski, K.; Piecuch, P. *J. Chem. Phys.* **2005**, *122*, 074107.
(112) Hirata, S.; Fan, P.-D.; Auer, A. A.; Nooijen, M.; Piecuch, P. *J. Chem. Phys.* **2004**, *121*, 12197.
(113) Møller, C.; Plesset, M. S. *Phys. Rev.* **1934**, *46*, 618.
(114) Dunning, T. H., Jr. *J. Chem. Phys.* **1989**, *90*, 1007.
(115) Kendall, R. A.; Dunning, T. H., Jr.; Harrison, R. J. *J. Chem. Phys.* **1992**, *96*, 6796.
(116) Frisch, M. J.; Trucks, G. W.; Schlegel, H. B.; Scuseria, G. E.; Robb, M. A.; Cheeseman, J. R.; Montgomery, J. A., Jr.; Vreven, T.; Kudin, K. N.; Burant, J. C.; Millam, J. M.; Iyengar, S. S.; Tomasi, J.; Barone, V.; Mennucci, B.; Cossi, M.; Scalmani, G.; Rega, N.; Petersson, G. A.; Nakatsuji, H.; Hada, M.; Ehara, M.; Toyota, K.; Fukuda, R.; Hasegawa, J.; Ishida, M.; Nakajima, T.; Honda, Y.; Kitao, O.; Nakai, H.; Klene, M.; Li, X.; Knox, J. E.; Hratchian, H. P.; Cross, J. B.; Adamo, C.; Jaramillo, J.; Gomperts, R.; Stratmann, R. E.; Yazyev, O.; Austin, A. J.; Cammi, R.; Pomelli, C.; Ochterski, J. W.; Ayala, P. Y.; Morokuma, K.; Voth, G. A.; Salvador, P.; Dannenberg, J. J.; Zakrzewski, V. G.; Dapprich, S.; Daniels, A. D.; Strain, M. C.; Farkas, O.; Malick, D. K.; Rabuck, A. D.; Raghavachari, K.; Foresman, J. B.; Ortiz, J. V.; Cui, Q.; Baboul, A. G.; Clifford, S.; Cioslowski, J.; Stefanov, B. B.; Liu, G.; Liashenko, A.; Piskorz, P.; Komaromi, I.; Martin, R. L.; Fox, D. J.; Keith, T.; Al-Laham, , M. A.; Peng, C. Y.; Nanayakkara, A.; Challacombe, M.; Gill, P. M. W.; Johnson, B.; Chen, W.; Wong, M. W.; Gonzalez, C.; Pople, J. A. *Gaussian 03*, Revision B.03; Gaussian, Inc., Pittsburgh, PA, 2003.
(117) Hehre, W. J.; Ditchfield, R.; Pople, J. A. *J. Chem. Phys.* **1972**, *56*, 2257.
(118) Hariharan, P. C.; Pople, J. A. *Theor. Chim. Acta* **1973**, *28*, 213.
(119) Clark, T.; Chandrasekhar, J.; Spitznagel, G. W.; Schleyer, P.v.R. *J. Comput. Chem.* **1983**, *4*, 294.
(120) Krishnan, R.; Binkley, J. S.; Seeger, R.; Pople, J. A. *J. Chem. Phys.* **1980**, *72*, 650.
(121) Sadlej, A. J. *Collect. Czech. Chem. Commun.* **1988**, *53*, 1995.
(122) Schmidt, M. W.; Baldridge, K. K.; Boatz, J. A.; Elbert, S. T.; Gordon, M. S.; Jensen, J. H.; Koseki, S.; Matsunaga, N.; Nguyen, K. A.; Su, S. J.; Windus, T. L.; Dupuis, M.; Montgomery, J. A. *J. Comput. Chem.* **1993**, *14*, 1347.

(123) Gordon, M. S.; Schmidt, M. W. In *Theory and Applications of Computational Chemistry: The First Forty Years*; Dykstra, C. E., Frenking, G., Kim, K. S., Scuseria, G. E., Eds.; Elsevier: Amsterdam, 2005; pp 1167−1190.
(124) Piecuch, P.; Kucharski, S. A.; Kowalski, K.; Musiał, M. *Comput. Phys. Commun.* **2002**, *149*, 71.
(125) ADF2009 suite of programs. Theoretical Chemistry Department, Vrije Universiteit, Amsterdam. http://www.scm.com
(126) Wesolowski, T. A.; Chermette, H.; Weber, J. *J. Chem. Phys.* **1996**, *105*, 9182.
(127) Casida, M. E.; Wesolowski, T. A. *Int. J. Quantum Chem.* **2004**, *96*, 577.
(128) Neugebauer, J. *J. Chem. Phys.* **2007**, *134*, 134116.
(129) Gritsenko, O. V.; Schipper, P. R. T.; Baerends, E. J. *Chem. Phys. Lett.* **1999**, *302*, 199.
(130) Dulak, M.; Wesolowski, T. A. *J. Chem. Phys.* **2006**, *124*, 164101.
(131) Jacob, C. R.; Beyhan, S. M.; Visscher, L. *J. Chem. Phys.* **2007**, *126*, 234116.
(132) McDowell, S. A. C.; Amos, R. D.; Handy, N. C. *Chem. Phys. Lett.* **1995**, *235*, 1.
(133) van Gisbergen, S. J. A.; Osinga, V. P.; Gritsenko, O. V.; van Leeuwen, R.; Snijders, J. G.; Baerends, E. J. *J. Chem. Phys.* **1996**, *105*, 3142.
(134) Guan, J.; Casida, M. E.; Köster, A. M.; Salahub, D. R. *Phys. Rev. B* **1995**, *52*, 2184.
(135) Vosko, S. H.; Wilk, L.; Nusair, M. *Can. J. Phys.* **1980**, *58*, 1200.
(136) Perdew, J. P.; Chevary, J. A.; Vosko, S. H.; Jackson, K. A.; Pederson, M. R.; Singh, D. J.; Fiolhais, C. *Phys. Rev. B* **1993**, *48*, 4978.